SPECIFIC HEAT NEAR THE NÉEL POINT IN THE $Mn_{1-c}\ Zn_c\ F_2$ SYSTEM

By

HADI SALAMATI-MASHHAD

Licentiate
University of Mashhad
Mashhad-Iran
1972

Master of Science
Oklahoma State University
Stillwater, Oklahoma
1977

Submitted to the Faculty of the Graduate College
of the Oklahoma State University
in partial fulfillment of the requirements
for the Degree of
DOCTOR OF PHILOSOPHY
May, 1981

SPECIFIC HEAT NEAR THE NÉEL POINT

IN THE $Mn_{1-c}\ Zn_c\ F_2$ SYSTEM

Thesis Approved:

George S. Dejon
Thesis Adviser

Larry E. Hallibunton

M. G. Rockley

Timothy M. Wilson

Norman N Durham
Dean of the Graduate College

ACKNOWLEDGMENTS

The author wishes to express his deep gratitude to his major adviser, Professor George S. Dixon, for his patient guidance and encouragement throughout this study, as well as his kind friendship shown during the author's stay at Oklahoma State University.

Appreciation is also expressed to the other Committee members, Dr. L. E. Halliburton, Dr. M. G. Rockley and Dr. T. M. Wilson for their assistance.

Finally, the author wishes to thank his wife, Mahboubeh, for her patience and understanding during the course of his research.

TABLE OF CONTENTS

LIST OF TABLES

LIST OF FIGURES

CHAPTER I

INTRODUCTION

Within the past few decades there has been a considerable advance both theoretically and experimentally in our knowledge of behavior of magnetic system in the vicinity of critical temperature.

The present experiment was designed to measure the specific heat of single crystal of the site random antiferromagnets in the system $Mn_{1-c}Zn_cF_2$ as a function of temperature and composition. The method of a.c. calorimetry will be used, and the emphasis will be on the shift in the Néel (transition) temperature as a function of composition and on the rate of increase in the specific heat as Néel temperature is approached. Results will be interpreted in the light of modern theories of phase transitions.

The most fundamental idea which helps elucidate the behavior near the critical point is the concept that this transition is describable by an order parameter (1-3), that measures the long-range or average degree of order in the system. It is zero in the high-temperature, disordered phase, and non-zero in the ordered phase. For a ferromagnet this order parameter is the spontaneous magnetization of the solid. The critical behavior of the properties of the system is dominated by short-range fluctuations in the local order. The average radius of such fluctuations is called the correlation length. At very high temperature the correlation length is close to zero, but as the temperature falls corre-

lations over larger distance begin to appear. As the temperature approaches the critical point the correlation length grows rapidly. One can measure this experimentally by scattering light (4) or thermal neutrons (5) from the fluctuations. The principle of scaling states that all the equilibrium critical properties follow from the variation of this correlation length with temperature and magnetic field, provided that the forces between atoms are short ranged.

It has been proposed that the critical behavior is independent of the nature of the interactions, if they are short ranged, but depend only on the dimensionality of the order parameter, i.e., whether it is a one, two, three or possibly higher dimensional vector. This proposal is called universality (6). If this is true, then the critical properties of all materials fall into a relatively small number of universality class, e.g., for magnet the magnetization is given by a scalar if there is a unique easy axis, by a two-dimensional vector if there is a unique hard axis, and by a three-dimensional vector if all axes for magnetization are equivalent.

These, then, are different universality classes for magnet, and the models describing them are called the Ising, X-Y, and Heisenberg model respectively. According to universality there can be three and only three, different forms of behavior in magnet.

Recently there has been some experimental evidence that as the temperature approaches critical temperature in a magnetic system one can see crossover-phenomena from the Heisenberg to Ising system (7, 8). These crossover-phenomena may cause a dramatic change in the thermal critical behavior, and it is believed to be due to finite anisotropy which may arise from the dipole interaction, anisotropy exchange, or

interaction of the magnetic ions with the crystal line electric field (9).

It may be worth mentioning a brief summary of theoretical models that have been used to predict the critical behavior close to transition temperature namely Molecular Field, Ising and Heisenberg models.

In 1907 just a few years after the pioneering experimental work of Curie, Hopkinson and others proposed a theory of ferromagnetism which he assumed that the constituent magnetic moments interact with one another through an artificial "Molecular Field" which is proportional to the average magnetization. More specific models of interacting magnetic moments were put forward some years later. These models have in common the feature that they assume the magnetic moment to be localized on fixed lattice sites and that they influence one another through pairwise interactions, with an energy that achieves its maximum value, when the moments are parallel.

Two particular forms of the interaction are particularly interesting to this day. In the first of these, due to Wilhelm Lenz but called Ising model (10), the magnetic moments are assumed to be classical one dimensional "sticks" capable of only two orientations. Thus the Ising model is the magnetic model analogous to the lattice-gas model of fluid system.

A second model, called the Heisenberg model, (11, 12) regards the magnetic moment as being related to "quantum-mechanical" three dimensional spin operators, and assumes that the energy is proportional to scalar product of these operators.

Although the original Weiss Model (Molecular Field Model) of a magnetic system is quite easy to solve exactly, neither the Ising model

nor the Heisenberg model has yielded as yet to an exact solution for a three-dimensional lattice. Nevertheless, these models appear to represent reasonable theoretical descriptions of certain physical systems, and therefore their continued study has provided us with considerable insight regarding magnetic phase transitions.

Some of the equilibrium properties of magnetic systems which are important in the description of a ferromagnet in the critical region are following.

1. The spontaneous magnetization versus temperature in zero external field which actually measure the order parameter in magnetic system.

2. The magnetic susceptibility, which measures the response of the magnetization to a change in applied magnetic field. This is related to the fluctuations in the order parameter by the fluctuation in dissipation theorem.

3. The specific heat, which measures the response of the energy to a change in temperature.

In the discussion which follows, we shall present the experimental data and the theoretical predictions now available on each of the properties listed above. In the view of the fact that each of these properties has an analogy in the liquid-gas system, as a consequence of universality law (13, 14), we shall make the connection between each magnetic property and its fluid analogy.

1. The Spontaneous Magnetization. In Figure 1 we present a schematic drawing of the temperature dependence of M(T) of a ferromagnet normalized to its value at T=O, (M(O), in zero external field (H=O). Along side this we present the fluid analogy, namely the temperature dependence of the liquid-gas density along the coexistance curve. In

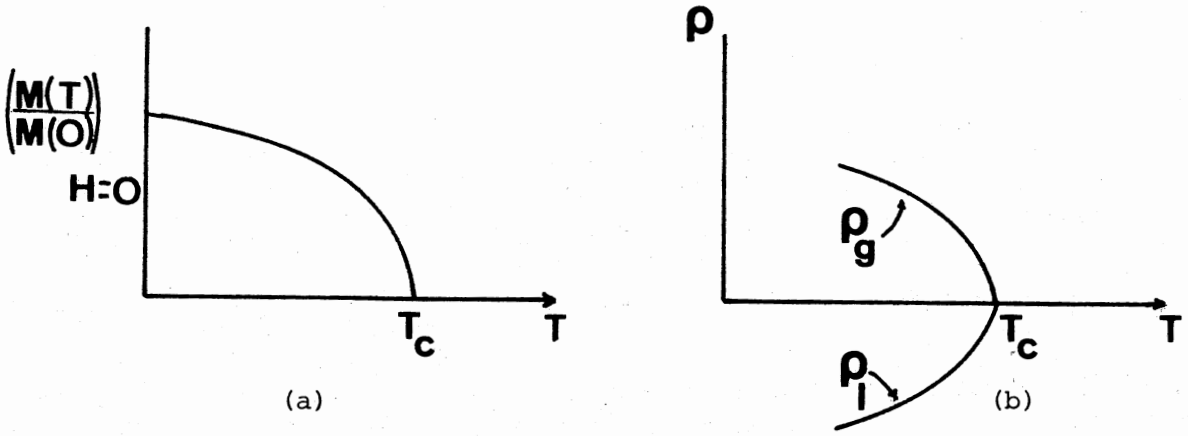

Figure 1. (a) A Schematic Plot of the Temperature Dependence of the Magnetization of a Ferromagnet. (b) The Fluid Analog: the Liquid and Gas Densities Along the Coexistence Curve

the critical region the magnetization and density data can be fit to equations of the form

$$\left(\frac{M(T)}{M(O)}\right)_{H=O} \equiv D\left(1 - \frac{T}{TN}\right)^{\beta} \qquad (1)$$

$$\left(\frac{\rho_L - \rho_g}{2\rho_c}\right) \equiv D'\left(1 - \frac{T}{TN}\right)^{\beta'} \qquad (2)$$

the first experimental measurement of D and β were reported in 1962 by P. Heller and G. Benedek (15) through a study of the nuclear resonance by F^{19} nucleus in the antiferromagnet MnF_2. In Table I we show the value for exponent which (1) was found to fit the data very well. These data show that $\beta = .333 \pm 0.003$. This is in disagreement with molecular field theories, which give $\beta = 1/2$ in the limit $T \to TN$. Heller and Benedek also carried out a careful investigation of the insulating ferromagnet EuS (16). The one-third power law was found to apply also to this system.

In Table I we also present the theoretical prediction of molecular field, Ising and Heisenberg models.

As an example of the analogous behavior of fluid we point out the work of Weinberger and Schneider (17, 13). They find that Equation (2) fits the data on Xenon very well in the vicinity of transition, this result is also shown in Table I.

2. The susceptibility. In Figure 2 we show the temperature dependence of the isothermal susceptibility of a ferromagnet as $T \to T_N$. Along side is shown the temperature dependence of the analogous property of the fluid, the isothermal bulk modulus along the critical isochore. The susceptibility of the ferromagnet is defined as

TABLE I

THE EXPERIMENTAL ESTIMATES OF CRITICAL EXPONENT ALONG WITH THE THEORETICAL PREDICTION OF EACH MODEL. n IS THE NUMBER OF DEGREE OF FREEDOM EXPECTED FOR ORDER PARAMETER

System	n	Critical Point Exponent					
		α,α'	Ref.	β	Ref.	γ,γ'	Ref.
Fluid							
Xe	1	$\alpha=\alpha'$ = .095	30	0.345 ± .015	13,17	$\gamma=\gamma'$ = 1.203	24
CO_2	1	$\alpha=\alpha'$ = .11	30	0.344	24	$\gamma=\gamma'$ = 1.20 ± .02	24
He^3	1	$\alpha=\alpha'$ = .105	31	.361	24	$\gamma=\gamma'$ = 1.15	24
Ferromagnet							
EuS	3	$\alpha=\alpha'$ = -0.044	32	0.33 ± 0.015	16		
Fe	3	$\alpha=\alpha'$ = -0.103	33	0.34 ± 0.02	27	γ = 1.13	22,20
						γ = 1.37 ± 0.04	23
						γ = 1.33 ± 0.04	25
Ni	3	$\alpha=\alpha'$ = -0.091	33	0.33 ± 0.02	27	γ = 1.35 ± 0.02	26
						γ = 1.29 ± 0.03	25
Antiferromagnet							
MnF_2	3			0.333 ± 0.003	15		
$RbMnF_3$	3	$\alpha=\alpha'$ = -0.135	33	0.316 ± 0.008	28	γ = 1.397	28
FeF_2	1	$\alpha=\alpha'$ = 0.135	34				
Theoretical Predictions							
Molecular Field Theory				0.5		γ = 1	
Ising Model	1	$\alpha=\alpha'$ = 0.125	35	0.3125	10	γ = 1.25	18
Heisenberg Model	3	$\alpha=\alpha'$ = -0.13	36	0.38 ± 0.03	29	γ = 1.33 ± 0.01	20,21

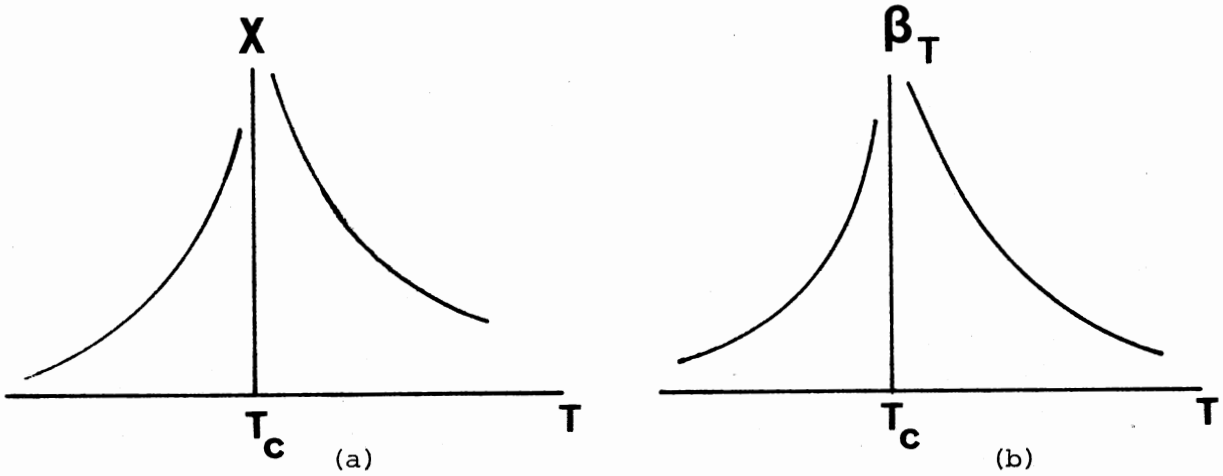

Figure 2. (a) The Temperature Dependence of the Isothermal Susceptibility of a Ferromagnet as $T \to T_c$. (b) The Temperature Dependence of the Isothermal Compressibility of a Fluid Evaluated at $p = p_c$ for $T > T_c$ and at $p = p_l$ or $p = p_c$ for $T < T_c$

$$\chi = (\partial M(T,H)/\partial H)_{H=0} . \tag{3}$$

As one approaches TN from the high temperature or paramagnetic side, χ diverge like

$$\underset{T \to T_N}{\chi} = \frac{C}{(T/T_N - 1)^{\gamma}} \qquad T > T_N \tag{4}$$

As one approaches T_N from the ferromagnetic side, χ can be fit to an equation of the same form as (4) but must leave the possibility that the coefficient C and exponent γ have different values for $T < T_N$. Thus, on this side of T_N we write

$$\underset{T_- \to T_N}{\chi} = \frac{C'}{(1 - \frac{T}{T_N})^{\gamma'}} \qquad T < T_N . \tag{5}$$

In the fluid the analogy is the isothermal compressibility β_T

$$\beta_T = \frac{1}{\rho} \left(\frac{\partial \rho}{\partial \rho}\right)_T . \tag{6}$$

As $T \to T_N$ from above, the compressibility at $\rho = \rho_c$ diverges as follows:

$$\underset{T_+ \to T_N}{\beta_{T,\rho_c}} = \frac{d}{(1 - \frac{T}{T_N})^{\gamma}} \qquad T > T_N \tag{7}$$

below T_N the relevant compressibility is that evaluated right at the co-existance line for either the liquid or gas.

$$\underset{(T_- \to T_N)}{\beta_{T,\rho_\ell \text{ or } \rho_g}} = \frac{d'}{(1 - \frac{T}{T_N})^{\gamma'}} . \tag{8}$$

we see that in the liquid case, the pressure plays the same role as does the magnetic field in ferromagnetic case.

The first comparison between the theoretical predictions (18-21) and experimental was provided by the work of Jacrot (22) who determined χ through a study of the scattering of neutrons from iron as $T \to T_N$ from above. His measurement indicated that $\gamma = 1.3$. Stimulated by the departure of γ from the classical value $\gamma = 1$, Noakes and Arrott (23) re-examined their older measurement of the susceptibility of iron for $T > T_N$, and they also carried out new measurement of this quantity. They found $\gamma = 1.37 \pm 0.04$. This result is also tabulated in Table I. The theoretical prediction of this exponent is also shown in Table I.

In the case of fluid, the classical theories give $\gamma = 1$, but the experimental measurement by Sengers (24) shows that $\gamma = 1.20 \pm 0.02$ for CO_2.

3. Specific Heat. The behavior of specific heat in the vicinity of critical point has received much theoretical and experimental attention for some years and it is the most difficult data to categorize and understand. The result of some experimental measurement of specific heat in the vicinity of critical region, which is frequently fit to expressions

$$C = \frac{A}{\alpha}\left(1 - \frac{T}{T_N}\right)^{-\alpha} + B \qquad T > T_N$$

$$= \frac{A'}{\alpha'}\left(1 - \frac{T}{T_N}\right)^{-\alpha'} + B' \qquad T < T_N \tag{9}$$

is given in Table I.

Also in Table I we include the theoretical prediction of the critical exponent for each correspondnet model.

In two dimensional Ising model, the specific heat behaves as

$$C = A \log \left|1 - \frac{T}{T_N}\right| + B \quad T > T_N$$
$$= A' \log \left|1 - \frac{T}{T_N}\right| + B' \quad T < T_N \tag{10}$$

with A = A' and B = B'. In molecular field theory, there is discontinuity in the specific heat. This corresponds to the result (10) in special case

$$A = A' = 0, \; B \neq B' .$$

All above descriptions was about pure magnetic system. Introduction of nonmagnetic impurity into a magnetic host behave as magnetic vacancies, their interaction with the spin of the magnetic ion are known to be zero. As the concentration (c) of nonmagnetic ions increases the Néel (transition) temperature decreases (37). At low c this fall off varies linearly with c, but as the concentration increases the deviation from linearity will increase, and goes to zero temperature at about 75% concentration (38, 39). This is expected to occur at c_o the critical concentration for the site percolation problem (40). For $c > c_o$ there are no infinite clusters of coupled magnetic ions in the crystal and therefore no long-range order. The results of neutron scattering experiments, and far-infrared observations (41, 42) are in good agreement with theoretical prediction of CPA (coherent potential approximation), which has been proposed by Buyers, Pepper and Elliott (39), and latter

has been improved by Coombs, Cowley and Holcomb (42). In this approximation method the nonmagnetic defect can be considered within the same framework as magnetic ion by introducing potential that will keep the magnetic ion spin wave from propagating via the nonmagnetic ion. In other words, one has to put the impurity-host and impurity-impurity interaction equal to zero and modify the coupling strength between the magnetic ion as well (43, 44).

CHAPTER II

EXPERIMENTAL PROCEDURE

The Sample

Manganese difluoride crystallizes in a tetragonal rutile structure (45), with two MnF_2 formula units in a primitive cell. In this structures each unit cell contains two manganese ions at the positions (0,0,0) and (1/2,1/2,1/2) and four fluoride ions at ± (U,U,0) and ± (1/2 + U, 1/2 - U, 1/2). The lattice constants of manganese difluoride are (46)

$$a = 4.8734 \pm 0.0002 \text{ Å}$$

$$c = 3.3099 \pm 0.0005 \text{ Å}$$

The value of U = 0.310 ± 0.003, and the density is 3.925 g cm^{-3}. The crystal structure of manganese difluoride is shown in Figure 3. The zinc difluoride also has a tetragonal rutile structure, with two ZnF_2 formula unit in a primitive cell. The lattice constant of zinc difluoride are (46)

$$a = 4.7034 \pm 0.0002 \text{ Å}$$

$$c = 3.1335 \pm 0.0003 \text{ Å}$$

and the value of U = 0.307 ± 0.003. The zinc doped sample of manganese difluoride grown in Oklahoma State University Crystal Growth Laboratory

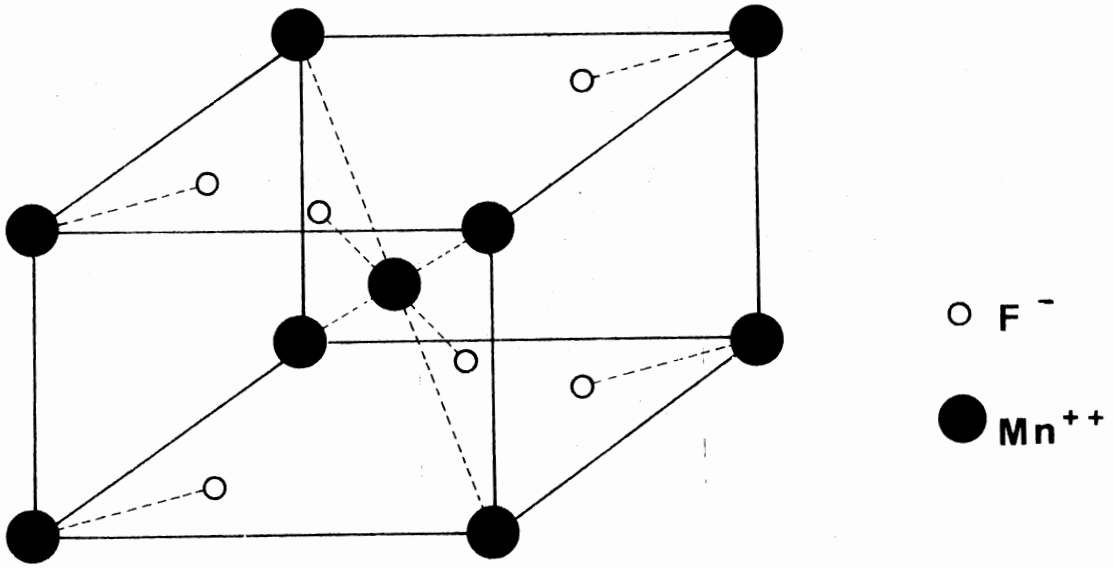

Figure 3. Crystal Structure of Manganese Difluoride

from stoichiometric mixtures of manganese difluoride and zinc difluoride by a Bridgman-Stockbarger technique. Details about the growth apparatus and procedure are given by Wolf (47).

Preparation of Sample

The samples were cut from the single crystal with a diamond saw into 4 x 10 mm rectangular plate and were thinned by polishing on #240 silicon carbide paper to a thickness about .5 mm.

Experimental Method

We have used the steady-state a.c. technique in our measurement of specific heat. The measurement of the specific heat of a substance by a.c. technique was introduced by Sullivan and Seidel (48) and by Handler, Mapother and Rayl (49).

In this method a sample of thickness L and cross-sectional area A is heated uniformly at one side (x = o) by a sinusoidal heat flux

$$\dot{q}(O,t) = \frac{Q^{O}}{2A} e^{i\omega t} \tag{11}$$

where Q^{O} is the amplitude of the heat and ω is the frequency of heater. The other side of the slab (x = b) is coupled uniformly to a bath at constant temperature Figure 4. Let the thermal conductivity of the sample be K, its specific heat c; and its density ρ. The thermal diffusivity η is defined by the relation

$$\eta = \frac{K}{\rho c}, \tag{12}$$

the characteristic length

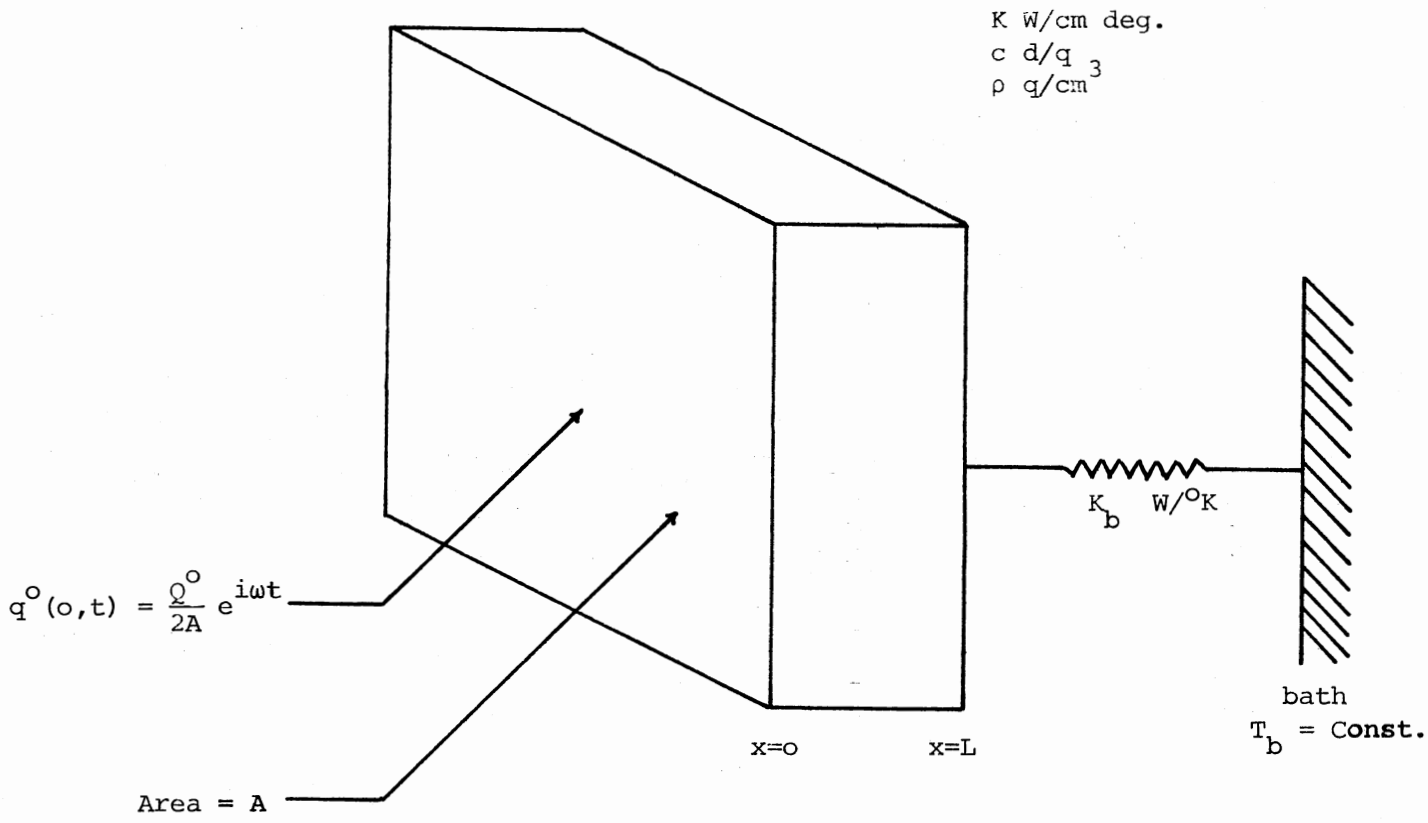

Figure 4. Slab-Shaped Sample of Thickness L Thermally Connected to a Bath at x = L and Having a Sinusoidal Heat Input Per Unit Area $q^o(o,t)$ at x = o

$$lo = \left(\frac{2\eta}{\omega}\right)^{1/2} . \qquad (13)$$

It has been assumed that, the heater at x = o and the thermometer at x = L are coupled to the sample with very short relaxation time.

By the application of the matrix method of expressing the temperature and heat flux at one point in terms of these quantities at another point (50), the oscillatory temperature dependence of sample at the position x = L is found approximately to be

$$T_{ac} = \frac{Q^{o}}{2\omega c} \qquad (14)$$

where c is the specific heat.

Under the condition that the sample thickness L is much smaller than the characteristic thermal length lo.

By measuring the T_{ac} and knowing the power input and the frequency one can find the specific heat c.

The relative merits of the a.c. technique for the measurement of the specific heat over conventional calorimetric techniques are briefly: (a) high resolution; (b) high sensitivity, (c) a continuous record of specific heat versus temperature, whereas using conventional techniques, one usually obtains a point by point record of specific heat versus temperature: (d) the small samples used provide better temperature uniformity and more uniform properties across the sample; (e) finally, the a.c. method forms the basis for the simultaneous measurement of the specific heat and other properties.

Apparatus

The complete apparatus consisted of a cryostat and sample holder and associated electronics. In addition there was the necessary equipment to evacuate the sample holder and to produce low temperatures by pumping liquid nitrogen. A calibrated resistance thermometer was used to measure the temperature. The circuit diagram for this measurement s shown in Figure 5. Figure 6 shows a schematic diagram of the cryostat and sample holder. The cryostat contains two pyrex glass vacuum dewars. They are: an exterior dewar to isolate the next interior dewar, the second dewar having a capacity 8.5 liters. In this container we put liquid nitrogen (LN_2) to cool the system. The outer dewar may be filled with LN_2 to use liquid helium in the inner dewar.

A detail of sample holder is shown in Figure 7. It is essentially a stainless steel vacuum can containing a heat sink, an ambient heater, a copper pot, and a brass circular plate, which holds the sample. This can is sealed from top and from this top emerges three stainless steel tubes. One of these is to take out the cable going to the meters and to the power sources. This tube is also used to evacuate the stainless steel can. The second tube is used to pump out the variable heat leak. This heat leak is used to increase the range in temperature that measurement can be made with a given cryogenic liquid. At the bottom this tube is connected to the brass pot. On the other side of the brass pot, there is a copper cylindrical heat sink which connect the sample plate to the brass pot. Above this there is an internal copper cylindrical heat sink that goes all the way through the second tube. A heat leaking chamber is left between the heat sink and the wall of the second tube. The chamber may be evacuated or may be filled with some gas. The set of

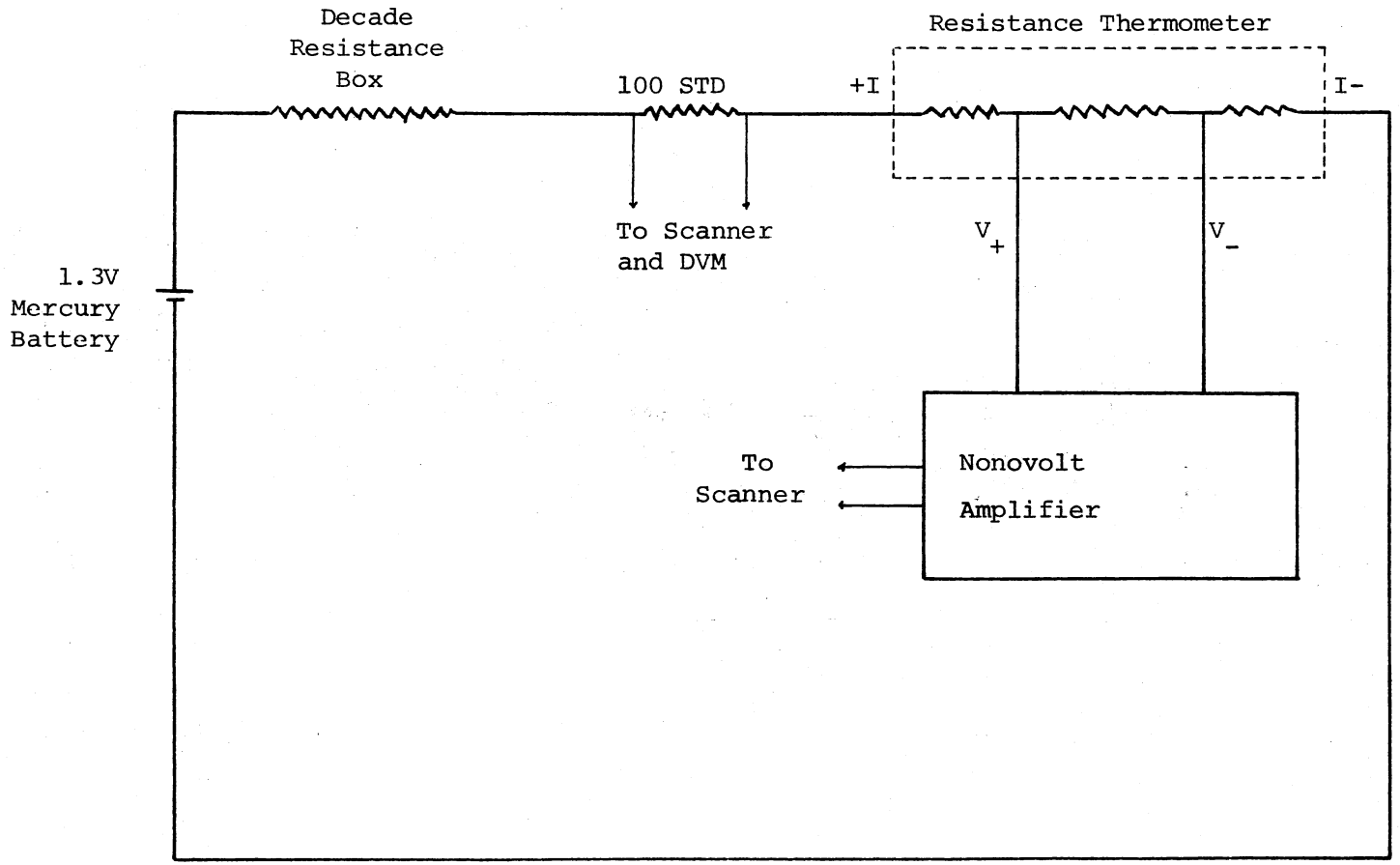

Figure 5. Circuit Diagram for Measuring the Calibrated Resistance Thermometer

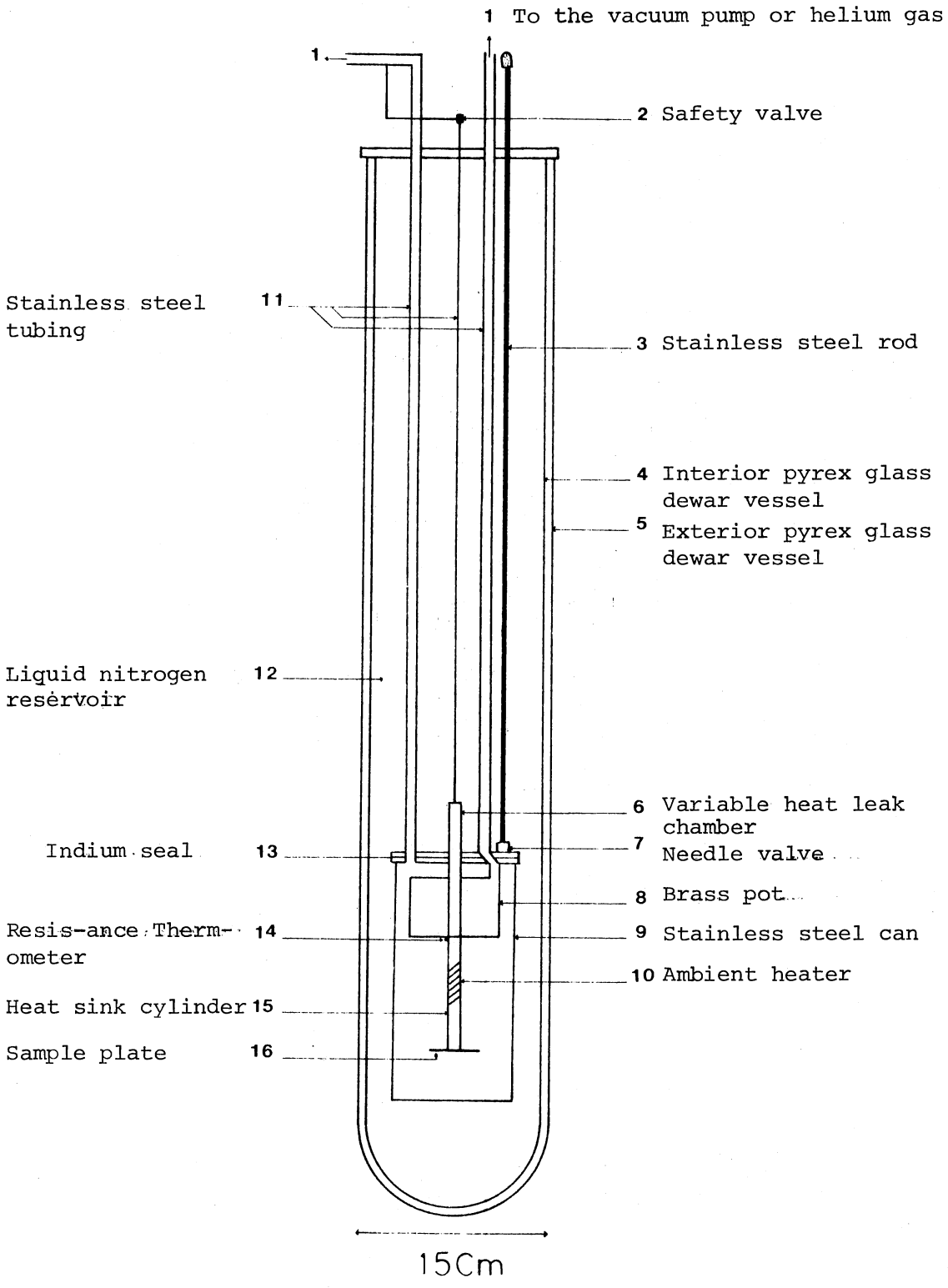

Figure 6. Cryostat and Sample Holder

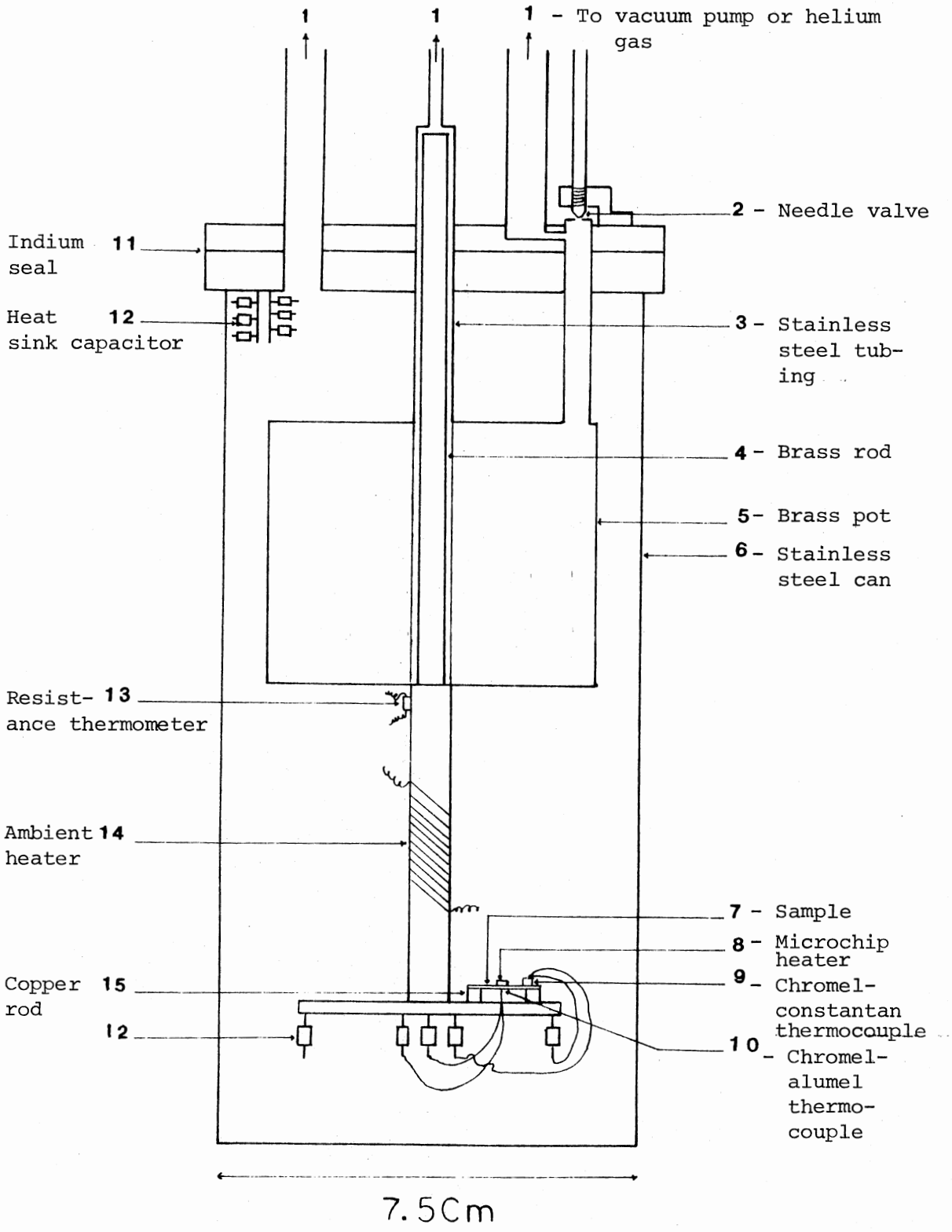

Figure 7. The Sample Holder

heat sink-heat leak works as a heat transfer cylinder from the inside of stainless steel can the cooler in the inner chamber of dewar or vice versa. The second heat transfer cylinder is connected to the exterior pumping system or to a connector to transfer gas into the cylinder when it is necessary. The brass pot was filled with liquid nitrogen by opening a needle valve and allowing liquid nitrogen to flow into the pot from the cryogenic bath in which the chamber was submerged. The third tube was used to pump this liquid nitrogen out. A temperature of about 50 K can be reached in this way.

The calibrated resistance thermometer was thermally mounted to the heat sink cylinder through a copper foil about 25 cm long and 2 cm wide. An ambient heater was made by wrapping teflon-coated constantan wire around the heat sink cylinder, and the temperature or the rate of increase in temperature could be controlled with this. At the end of this cylinder a circular plate with four holes was placed. The sample was glued to the plate via two copper bars using GE-7031 varnish. On the top of the sample there was a microchip heater and a constantan-alumel thermocouple. On the other side of the sample a 1 mil chromel-alumel thermocouple was placed.

The thermocouples and the microchip heater were glued to the sample by GE-7031 varnish. All the leads were thermally connected to the chamber by 15 pf silver-mica capacitors, and the leads connecting the terminals to the top of the probe were carefully twisted in pairs, shield and routed to avoid pick-up noise.

In all phase of pumping, the pumping speed was controlled by means of throttle valves.

Technique

Once the sample holder was inside of the dewar and the stainless steel can and brass pot have been evacuated and the leak check has been made, the liquid nitrogen was transferred to the inner dewar. Then the power was turned on in the microchip heater. The system then usually left over night to reach thermal equilibrium. By opening the needle valve and letting liquid nitrogen in the brass pot, then pumping this liquid nitrogen about two hours, a temperature of about 50 K degrees was reached. After about an hour sitting at almost 50 K degrees the throttle valve was partially closed, and the system was let to warm up by itself. The rate of increase in temperature is about 4 K degrees per hour that can be controlled by throttle valve. The signal picked up by the chromel-alumel thermocouple was transferred via a pre-amp (PAR^{TM} 113) to the lock-in amplifier (ITHACO Dynatrac 391A) which was recorded directly by the (Hits Altair 8800a computer) on a cassette tape.

The signal from constantan-chromel thermocouple which read the difference of temperature between the sample and sample holder was also recorded on cassette tape via (Keithley 174 Digital Multimeter), and finally the temperature inside the can was recorded on the cassette tape. All of these data were first transferred by a Keithley 702 scanner that has ten channels. Recording of these data was controlled by a computer program which is given in Appendix A. The frequency of signal generator in microchip heater was .15 H and the time constant on lock-in amplifier was 125 second. The block diagram of the electronics used to measure the heat capacity is shown in Figure 8. In calculation of temperature by a resistance thermometer which was calibrated by Lake Shore Cryo-

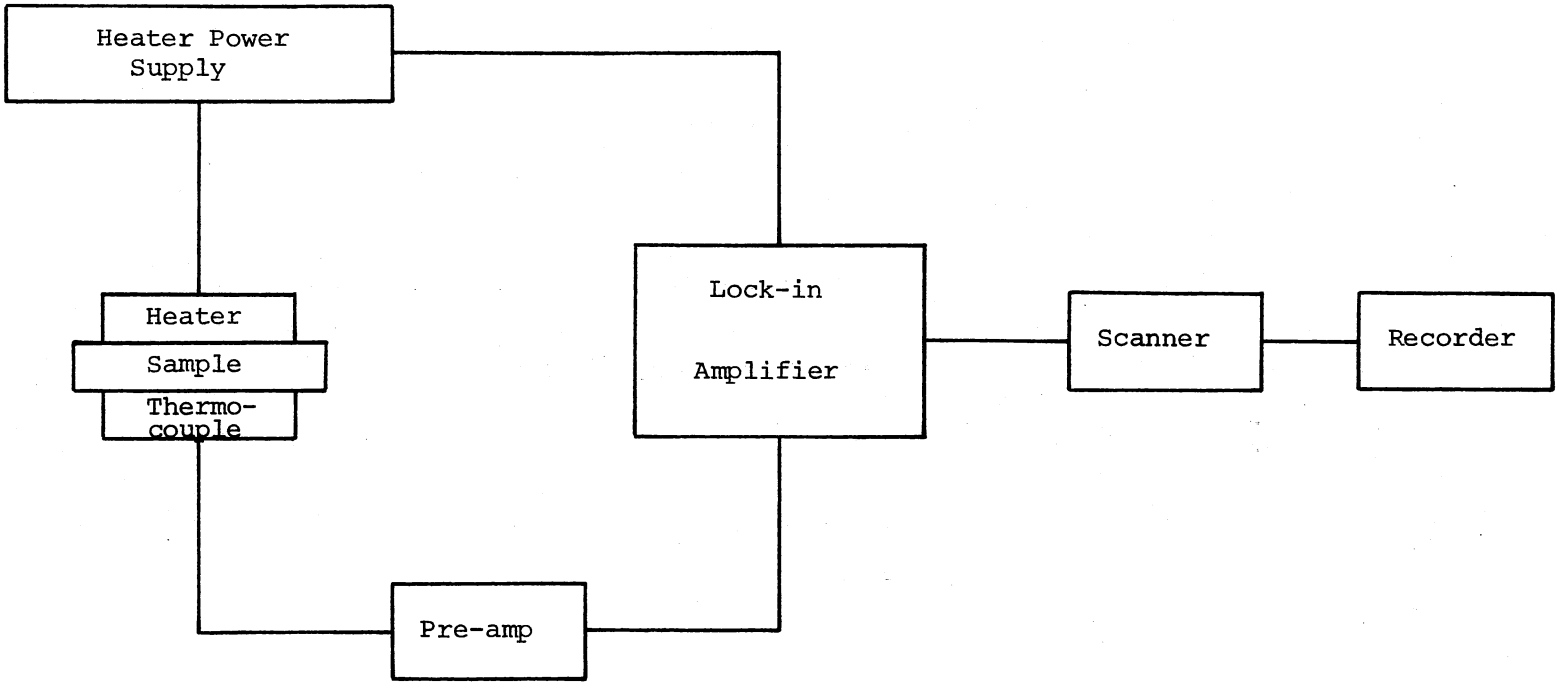

Figure 8. Block Diagram of the Electronics Used to Measure the Specific Heat

tronic, Inc., the change in temperature versus the change in resistance could be calculated from

$$T = (AR) + (BR)\ [\text{LOG } R] + (CR)\ [\text{LOG } R]^3 + (DR)\ [\text{LOG } R]^5 \qquad (15)$$

the sensitivity of this thermometer is good enough that one can measure temperature up to 10 millidegrees. The calculation for constan-chromel is also by the assumption that the temperature can be expanded in terms of emf in the following Equation

$$T = (AT) + (BT)V + (CT)V^2 + (DT)V^3 \ . \qquad (16)$$

The coefficients calculated for these equations is given in Table II and also the computer program of calculating specific heat is given in Appendix (B).

TABLE II

CALCULATED VALUE OF THE COEFFICIENTS FOR TEMPERATURE MEASUREMENT

Coefficient	Calculated Value
AR	$1.686466337 \times 10^{-1}$
BR	$-9.102717295 \times 10^{-2}$
CR	$4.758946594 \times 10^{-3}$
DR	$-7.747302235 \times 10^{-5}$
AT	8147.51561
BT	- 2702.213312
CT	305.9191829
DT	-11.71648754

CHAPTER III

EXPERIMENTAL RESULTS

The specific heat of one undoped and five different zinc-doped samples of manganese difluoride single crystals were measured from 50 to 80K.

The specific heat measured consists of a contribution from the spin system, and the lattice. So, in order to calculate the heat capacity associated with the antiferromagnetic ordering in mangenese difluoride, it is necessary to subtract from the experimentally measured quantities the contributions arising from the lattice vibrations (51, 52). This has been done by assuming that the change in the lattice contribution at this range of temperature is approximately linear. So we calculated the slope of specific heat of ZnF_2 versus temperature at this range of temperature and subtract the calculated value for this specific heat from our measured value. The results are shown in Figure 9, where we plot the magnetic specific heat versus temperature. As the rate of concentration of zinc increases the Néel (transition) temperature will decrease. The corresponding transition temperature for different zinc concentration is shown in Table III. The magnitude of specific heat is also decreased and the peak becomes wider. Figure 10 shows the relation between the concentration and the transition temperature. It seems that the relation between the concentration and the transition temperature is linear over the range of concentrations studied here.

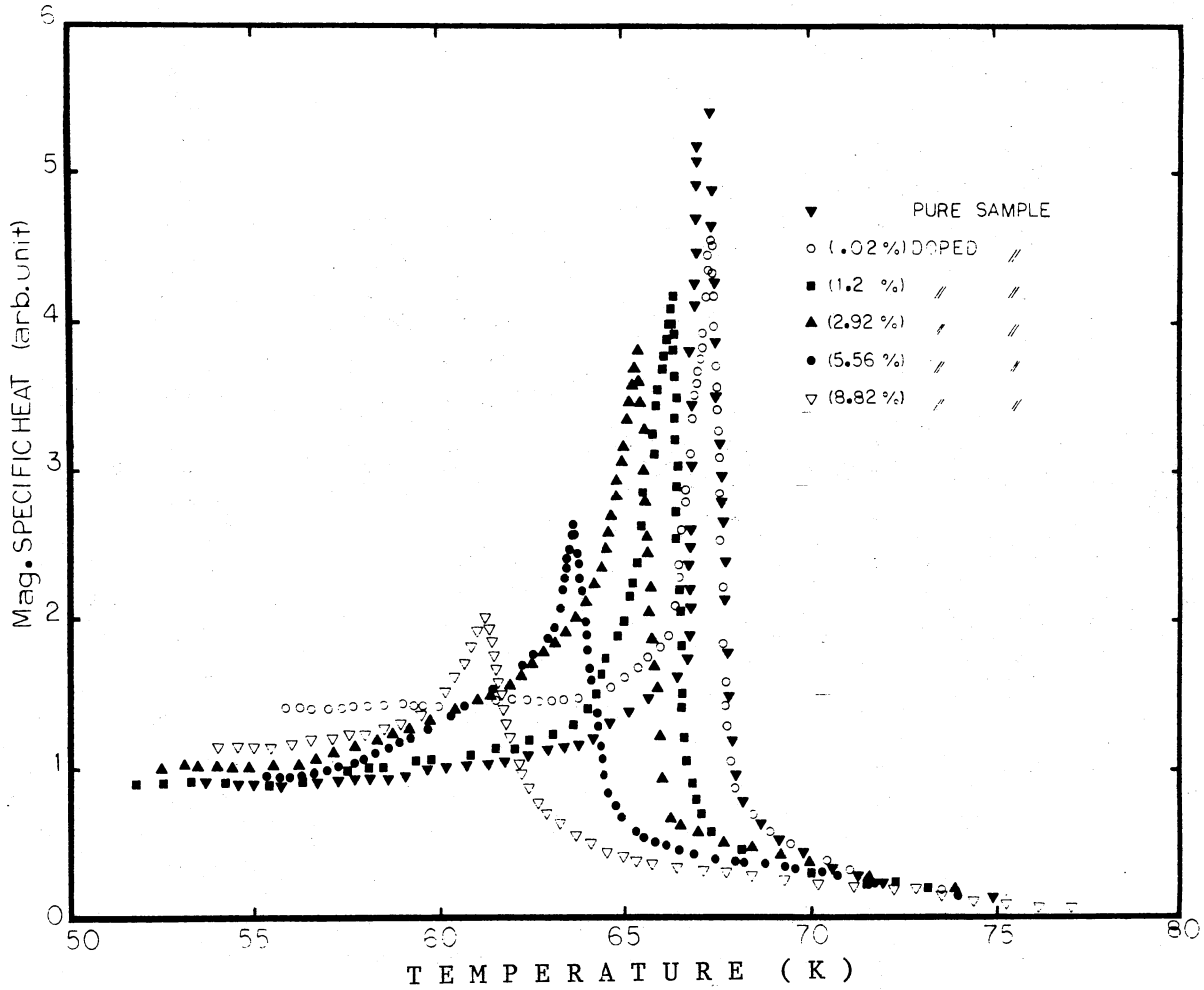

Figure 9. Mag. Specific Heat Versus Temp.

TABLE III

TRANSITION TEMPERATURE FOR DIFFERENT CONCENTRATIONS OF ZINC

Zinc Concentration (%)	Transition Temperature (K)
0	67.33
0.02	67.30
1.2	66.36
2.92	65.37
5.56	63.67
8.82	61.28

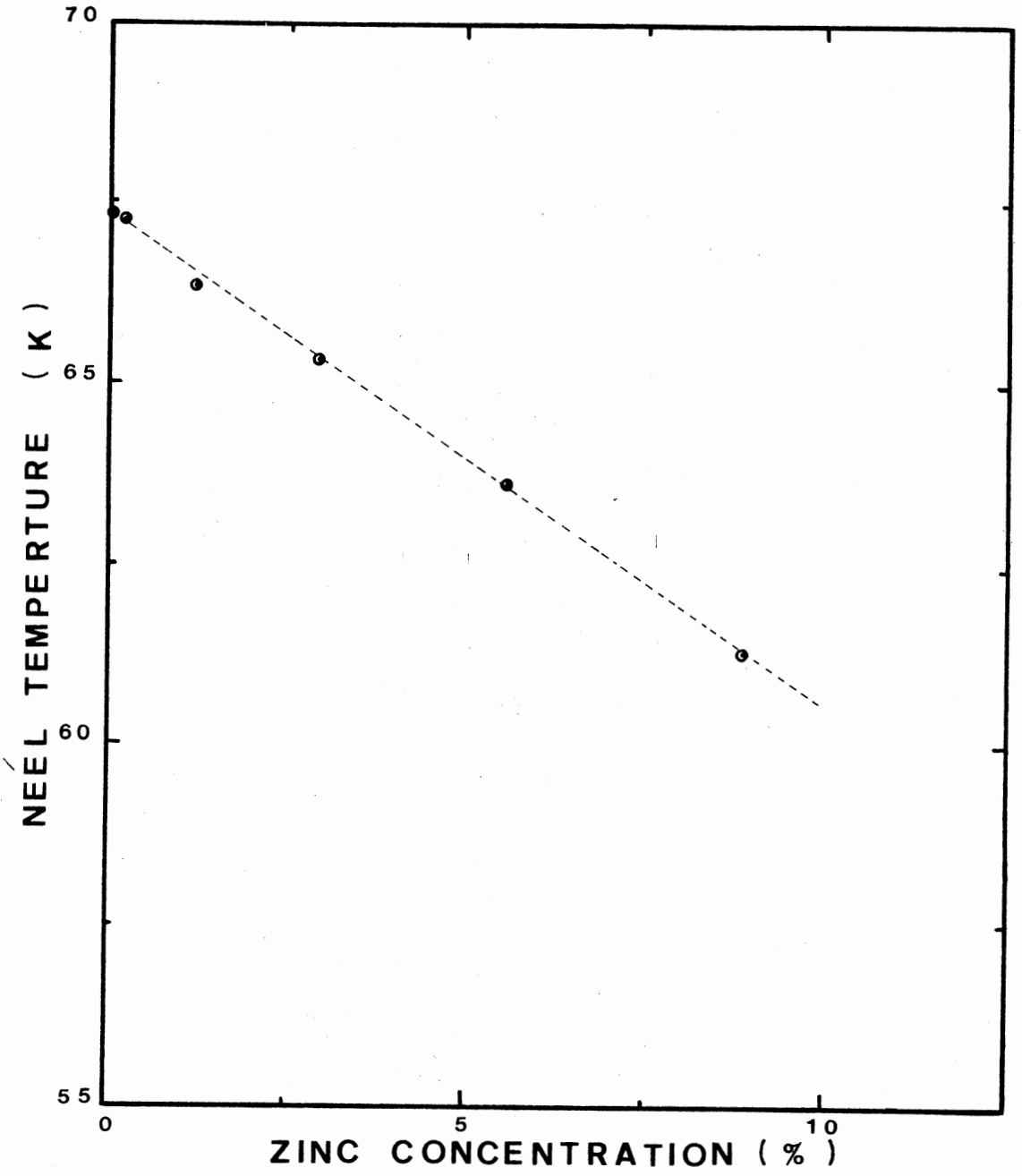

Figure 10. Néel Temp. for Different Concentrated Samples

CHAPTER IV

ANALYSIS AND DISCUSSION

First an attempt was made to fit the magnetic specific heat data in the vicinity of the critical point to a function of the type

$$C = \frac{A}{\alpha} (t)^{-\alpha} + B \qquad T > TN \tag{17a}$$

$$C = \frac{A'}{\alpha'} (t)^{-\alpha'} + B' \qquad T < TN \tag{17b}$$

where $t = \frac{T-TN}{TN}$ which should describe the assymptotic behavior as $T \rightarrow TN$. The result of this fit for all samples is shown in Figures 11-15. We find that it is impossible to find one value of the exponent to fit all of the data. The data are rounded due to presence of the Zn impurities so that it is not possible to make any clear determination of α by excluding data from TN. Second we tried to include corrections to scalling by fitting the data for lightly doped samples to a function of the type

$$C = \frac{A}{\alpha} t^{-\alpha} (1+Dt^{x}) + B \qquad T > TN \tag{18a}$$

$$C = \frac{A'}{\alpha'} t^{-\alpha'} (1+D't^{x}) + B' \qquad T < TN \tag{18b}$$

which was proposed by Ahlers and others (35, 53). The term Dt^{x} repre-

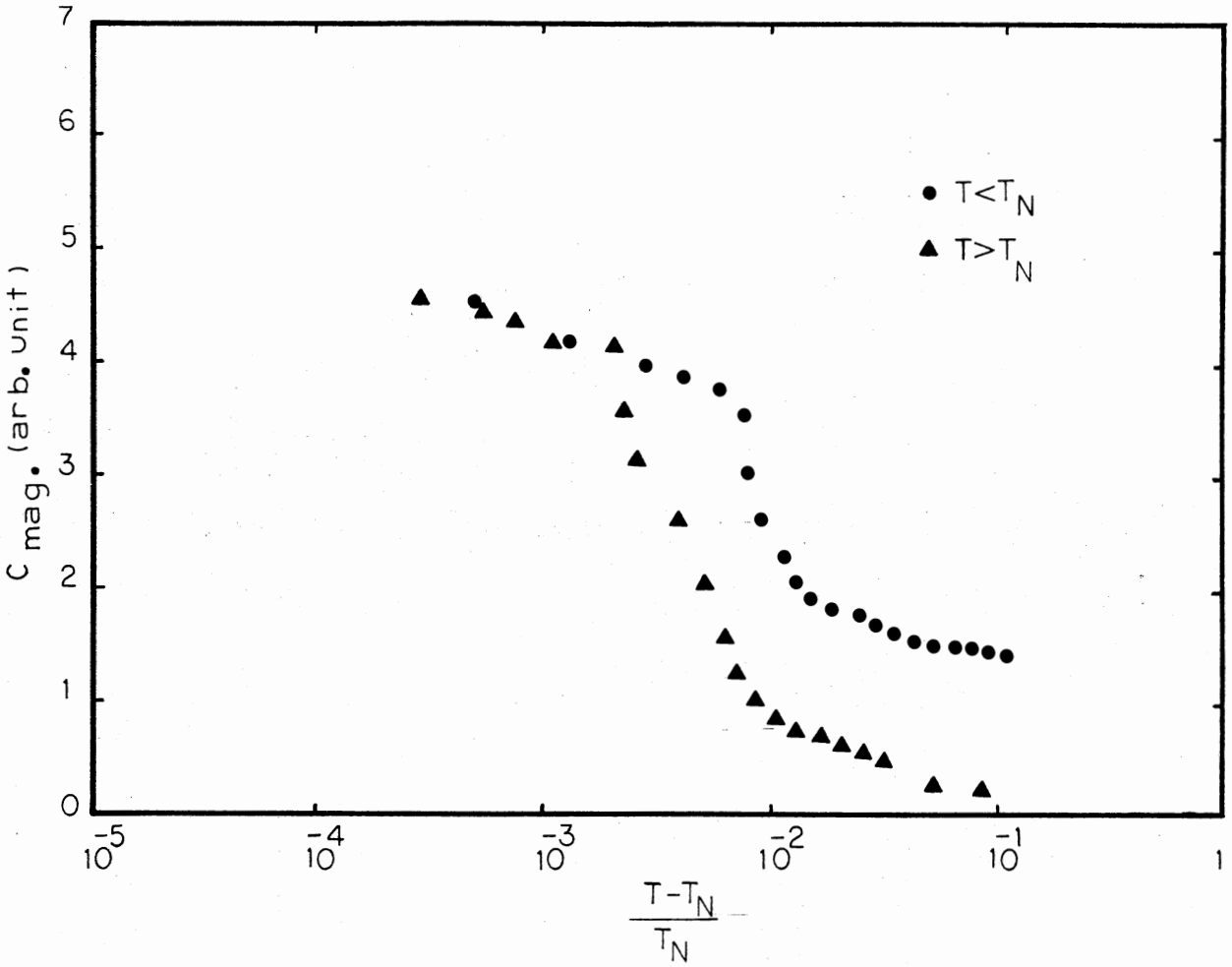

Figure 11. A Semi-log Plot of Mag. Specific Heat of 0.02% Zinc Dope Sample

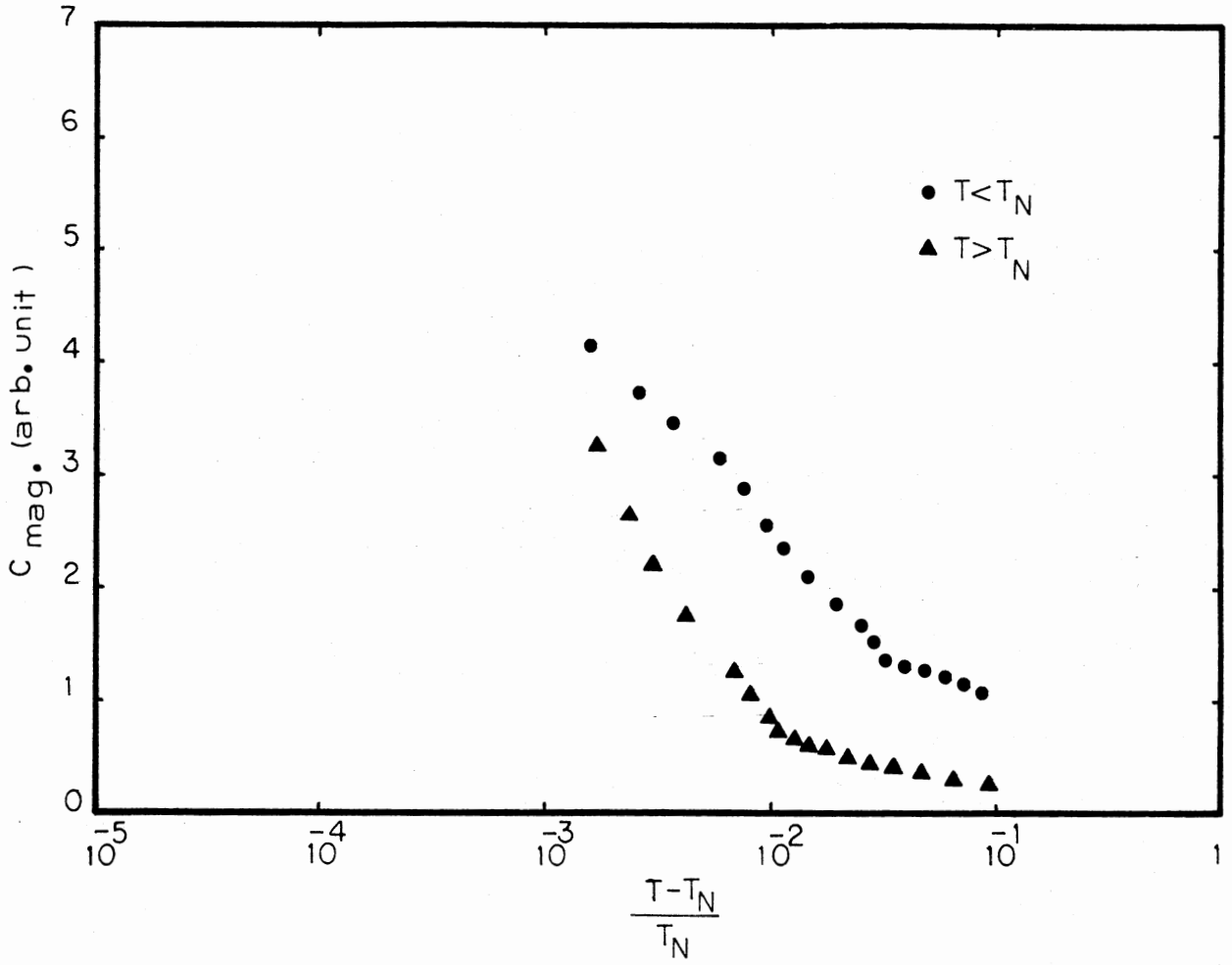

Figure 12. A Semi-log Plot of Mag. Specific Heat of 1.2% Zinc Doped Sample

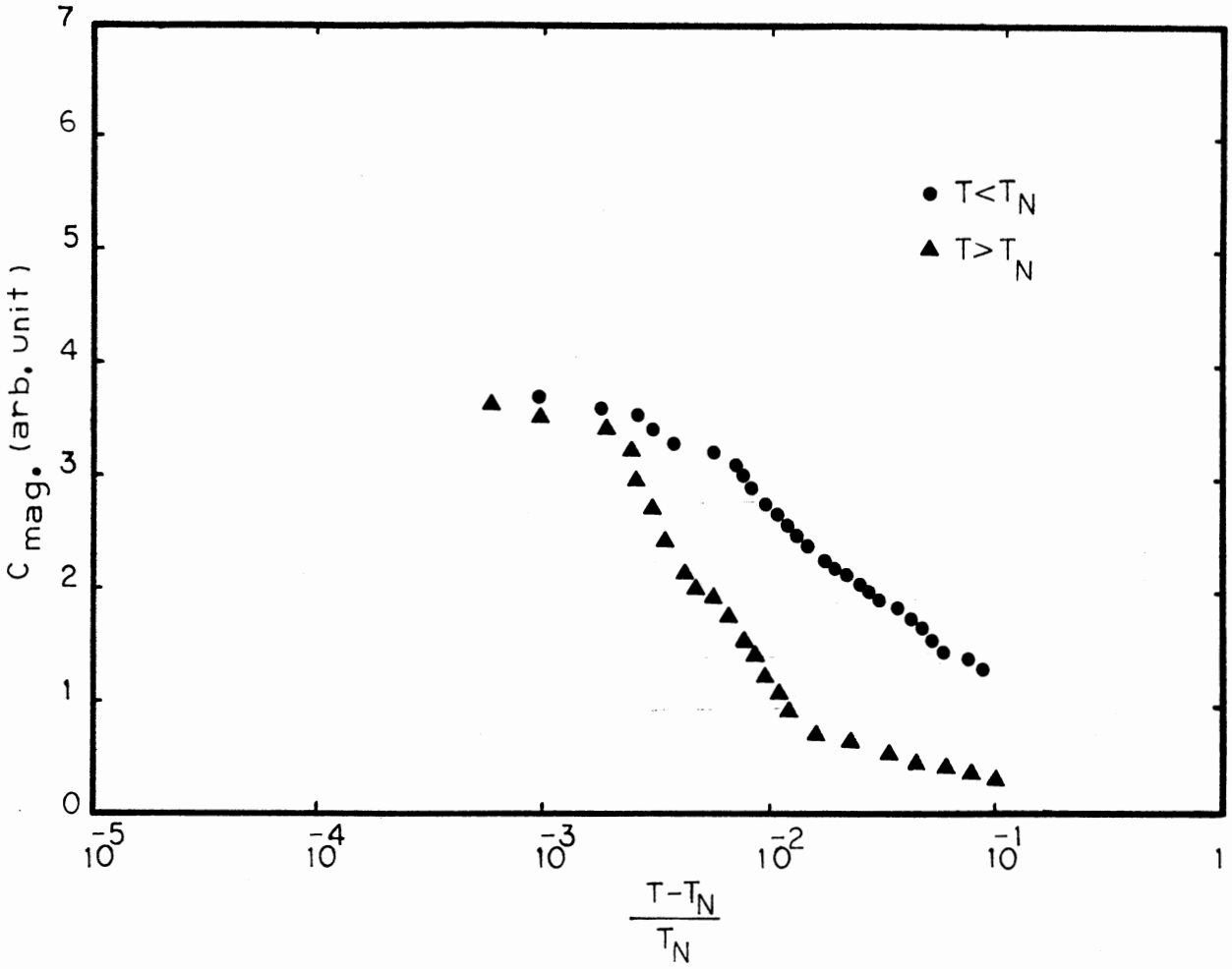

Figure 13. A Semi-log Plot of Mag. Specific Heat of 2.92% Zinc Doped Sample

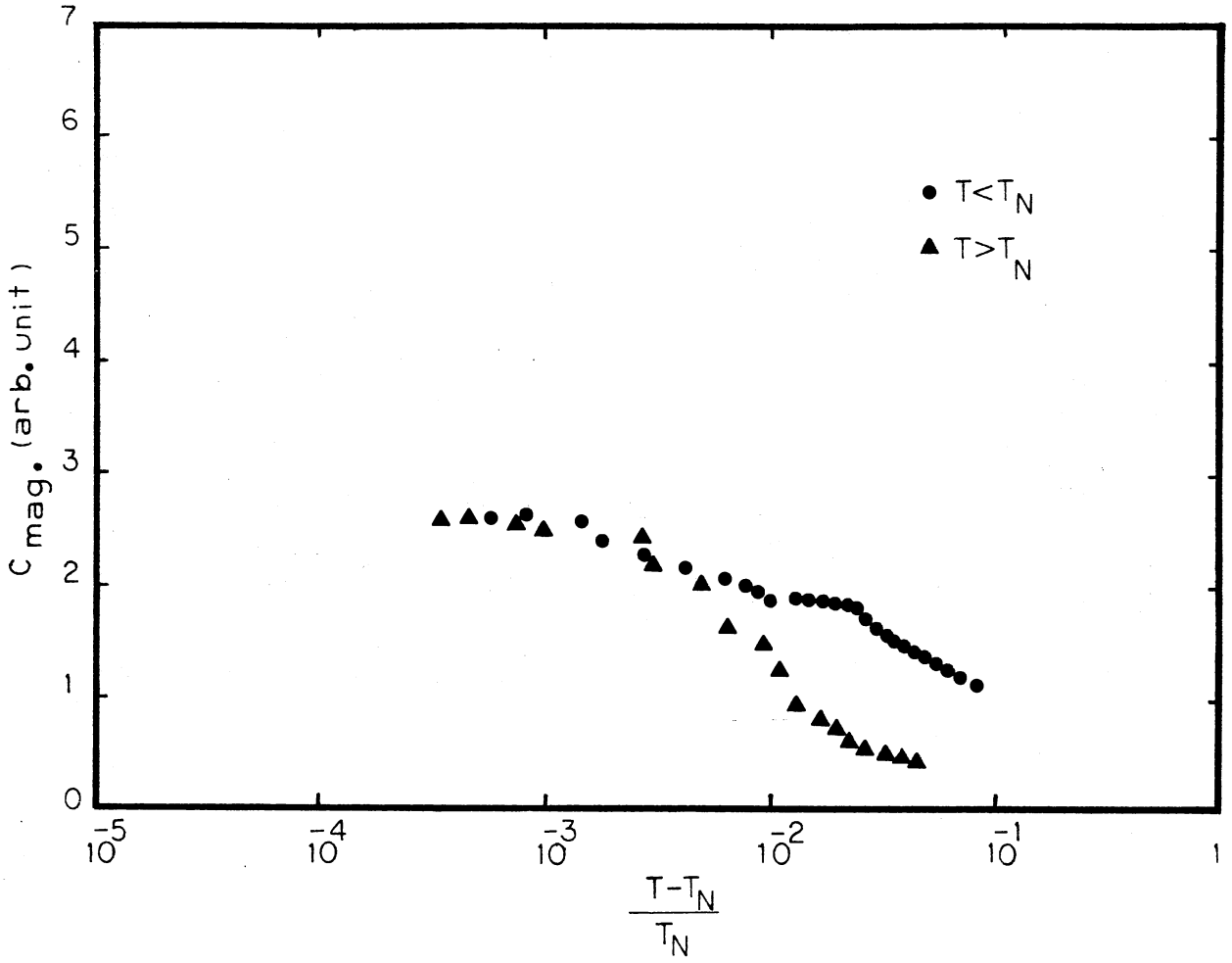

Figure 14. A Semi-log Plot of Mag. Specific Heat of 5.56% Zinc Doped Sample

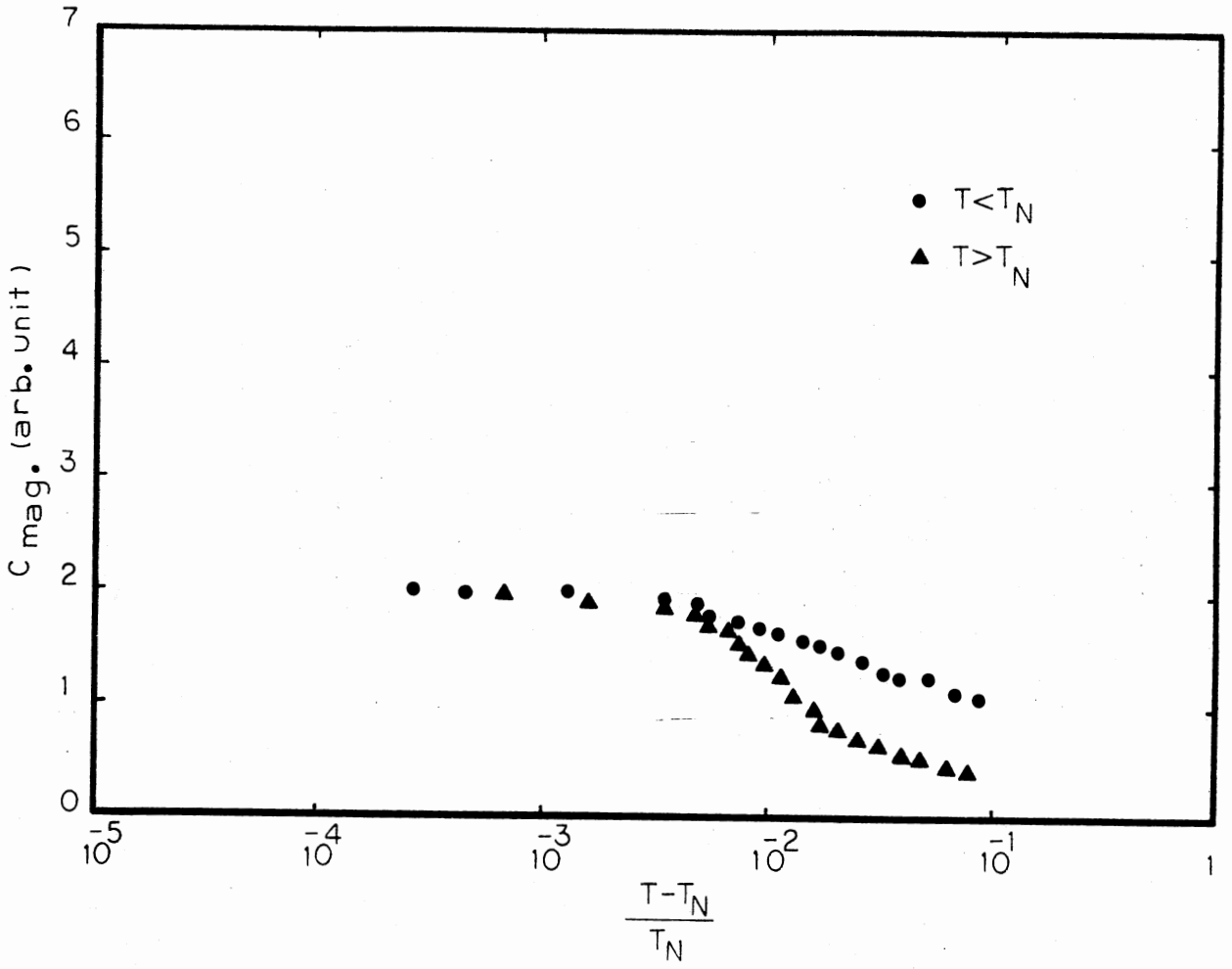

Figure 15. A Semi-log Plot of Mag. Specific Heat of 8.82% Doped Sample

sent the lowest order correction to scalling which vanishes at t = o. In fitting the data we imposed the scalling constraints

$$\alpha = \alpha' \tag{19a}$$

$$x = x' \, . \tag{19b}$$

The series expansion (54) calculations indicate that x is not strongly dependent on the spin dimensionality n and yield a result consistent with $x = x' = 0.5 \pm 0.02$ for the first order correction to scaling. We have used the previously founded values by Landau (55) for parameters

$$x = x' = 0.5 \pm 0.01$$

$$D = - D' = 0.25$$

and assumed that $\alpha = \alpha' = 0.125$ which is predicted by Ising model. This is expected to apply assymatically to MnF_2 since it has a unique easy axis. The results for this type of assumption for lightly doped samples are shown in Figures 16-18, where we plot magnetic specific heat versus

$$Z_I = (t)^{-0.125} \left[1 \pm 0.25 \, (t)^{0.5}\right] \, .$$

These results show a very good straight line behavior close to transition temperature and a break in the behavior about $Z_I = 1.42$ ($t \approx 4 \times 10^{-2}$) for $T < TN$ and about $Z = 1.83$ ($t \approx 10^{-2}$) for $T > TN$.

In another way we assume all of the parameter to be the same as above and tried for $\alpha = \alpha' = - 0.14$ which is the predicted value for exponent by Heisenberg model. The result of this type of asssumption for lightly doped samples is shown in Figures 19-21, where we plot the

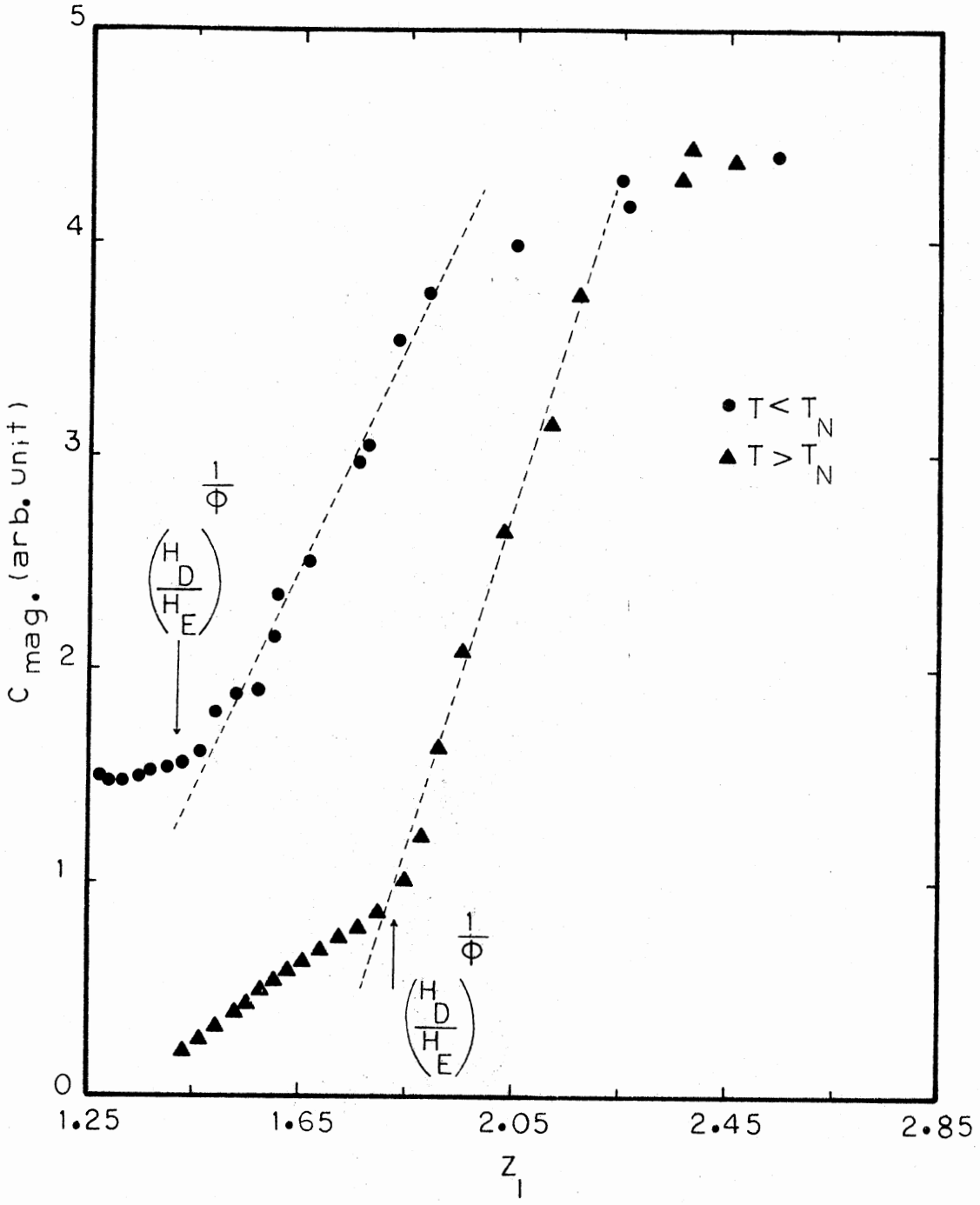

Figure 16. Mag. Specific Heat for 0.02% Zinc Doped Sample Versus $Z_I = (t)^{-0.125}\,[1 \pm 0.25(t)^{0.5}]$ Assuming Ising-Behavior

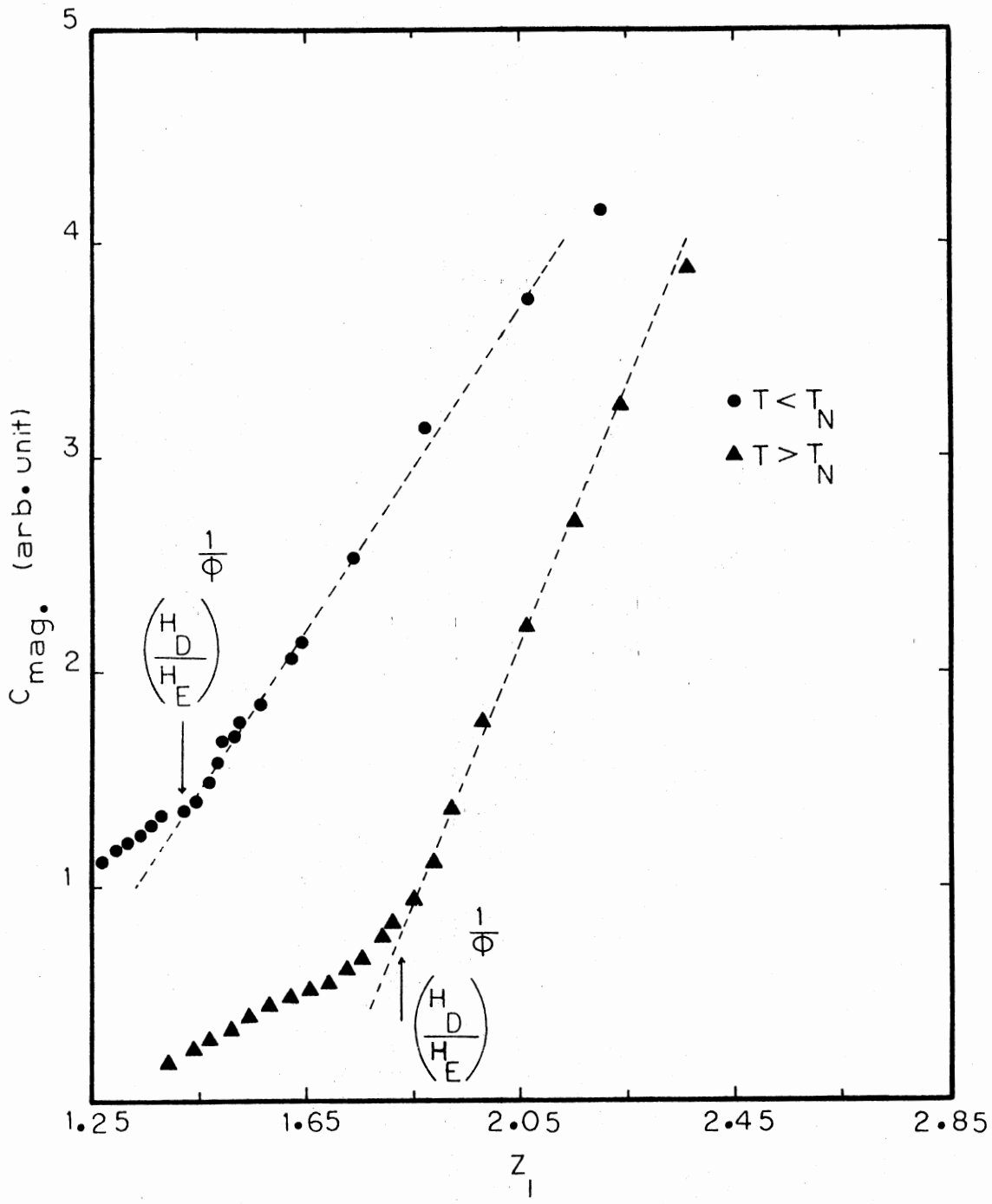

Figure 17. Mag. Specific Heat for 1.2% Zinc Doped Sample Versus $Z_I = (t)^{-0.125}\ [1 \pm 0.25(t)^{0.5}]$ Assuming Ising-Behavior

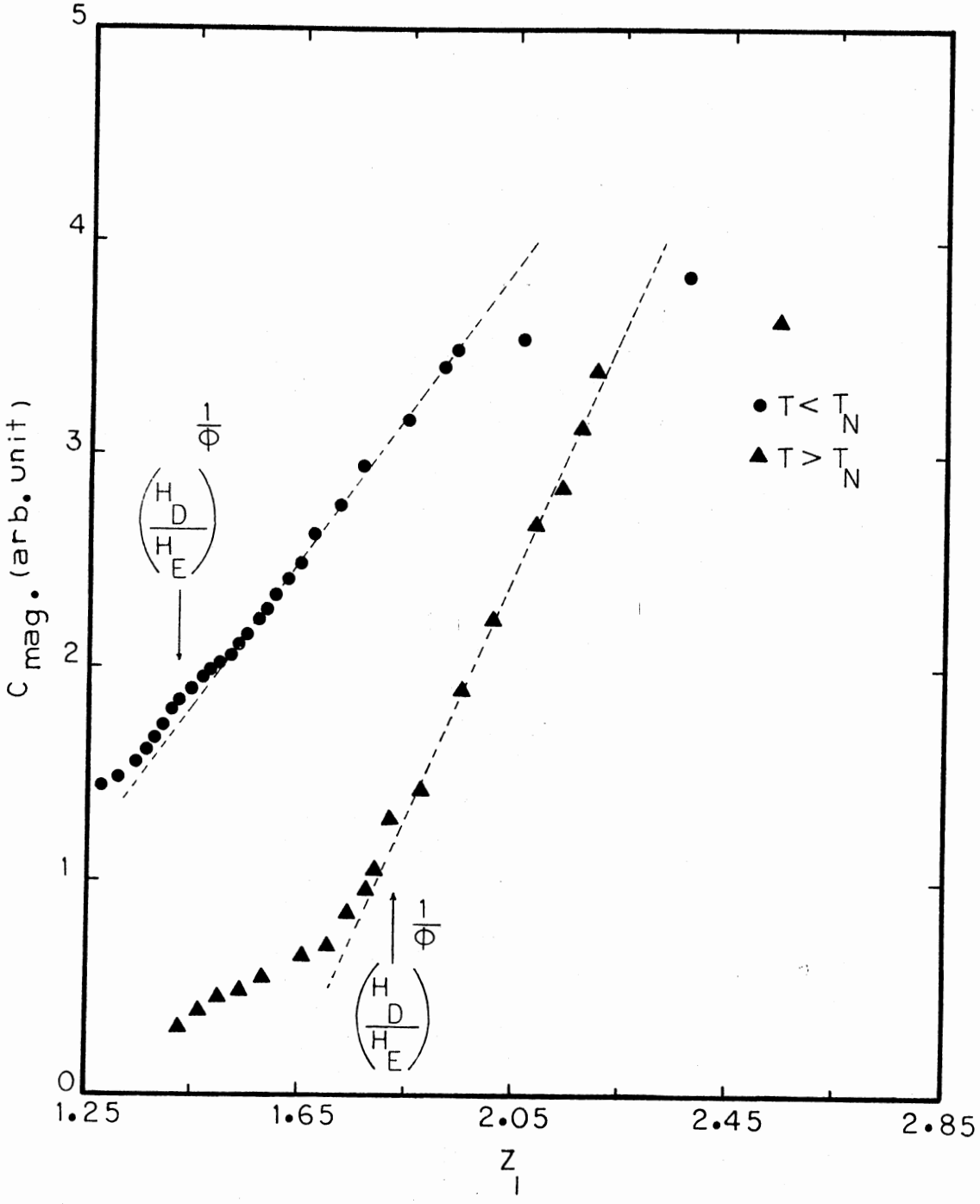

Figure 18. Mag. Specific Heat for 2.92% Zinc Doped Sample Versus $Z_I = (t)^{-0.125}\,[1 \pm 0.25(t)^{0.5}]$ Assuming Ising-Behavior

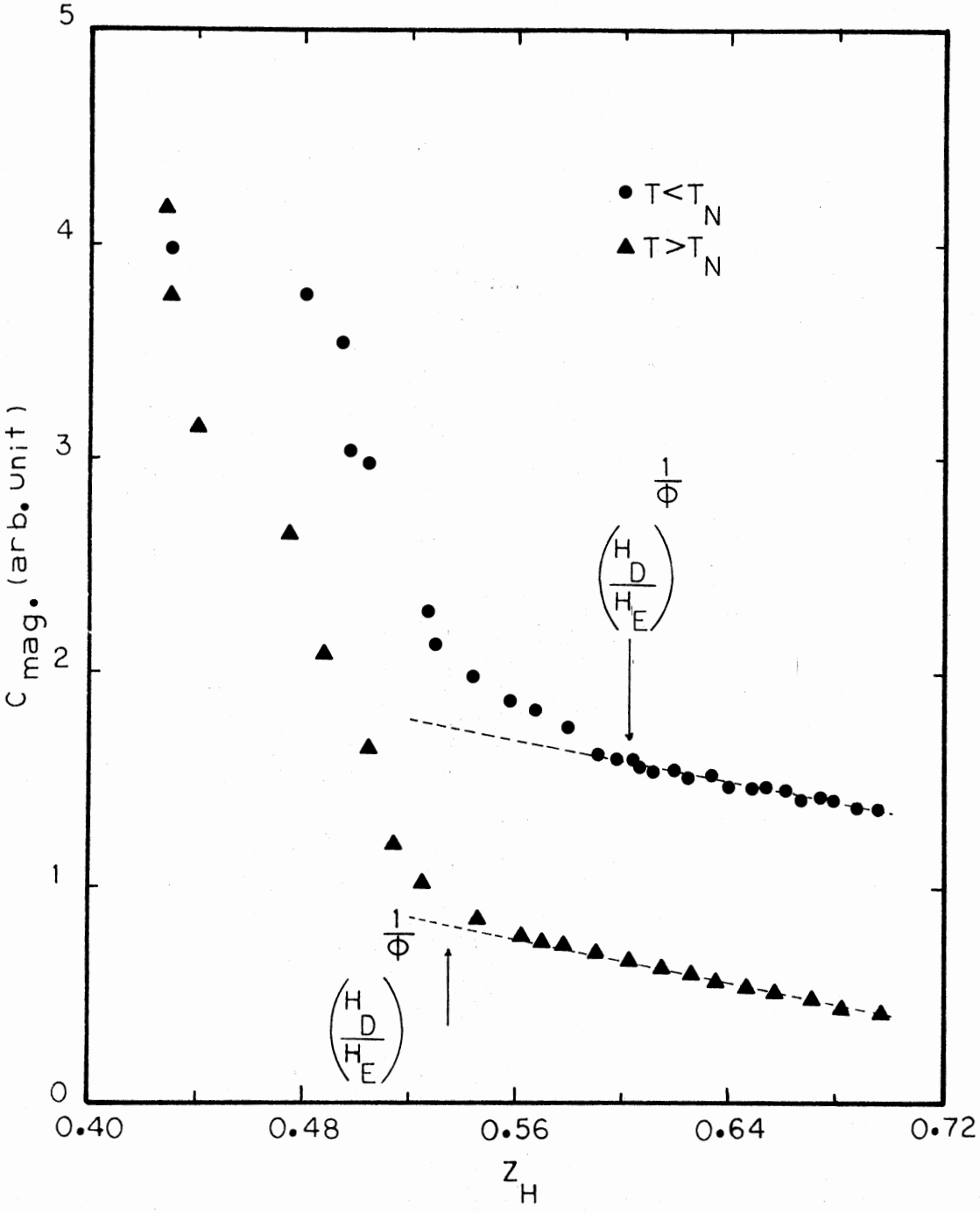

Figure 19. Mag. Specific Heat for 0.02% Zinc Doped Sample Versus $Z_H = (t)^{0.14}\,[1 \pm 0.25(t)^{0.5}]$ Assuming Heisenberg-Behavior

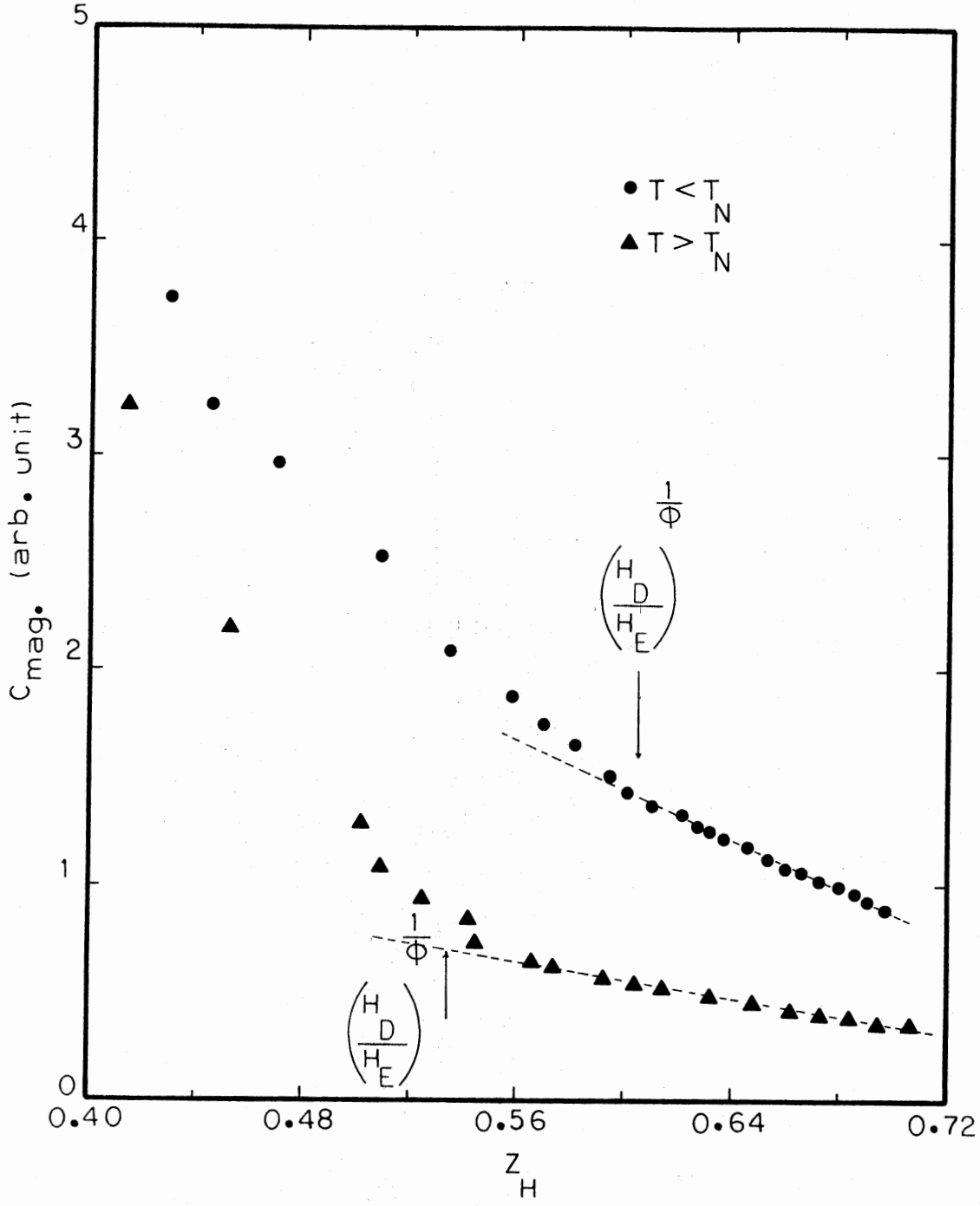

Figure 20. Mag. Specific Heat for 1.2% Zinc Doped Sample Versus $Z_H = (t)^{0.14}\,[1 \pm 0.25(t)^{0.5}]$ Assuming Heisenberg-Behavior

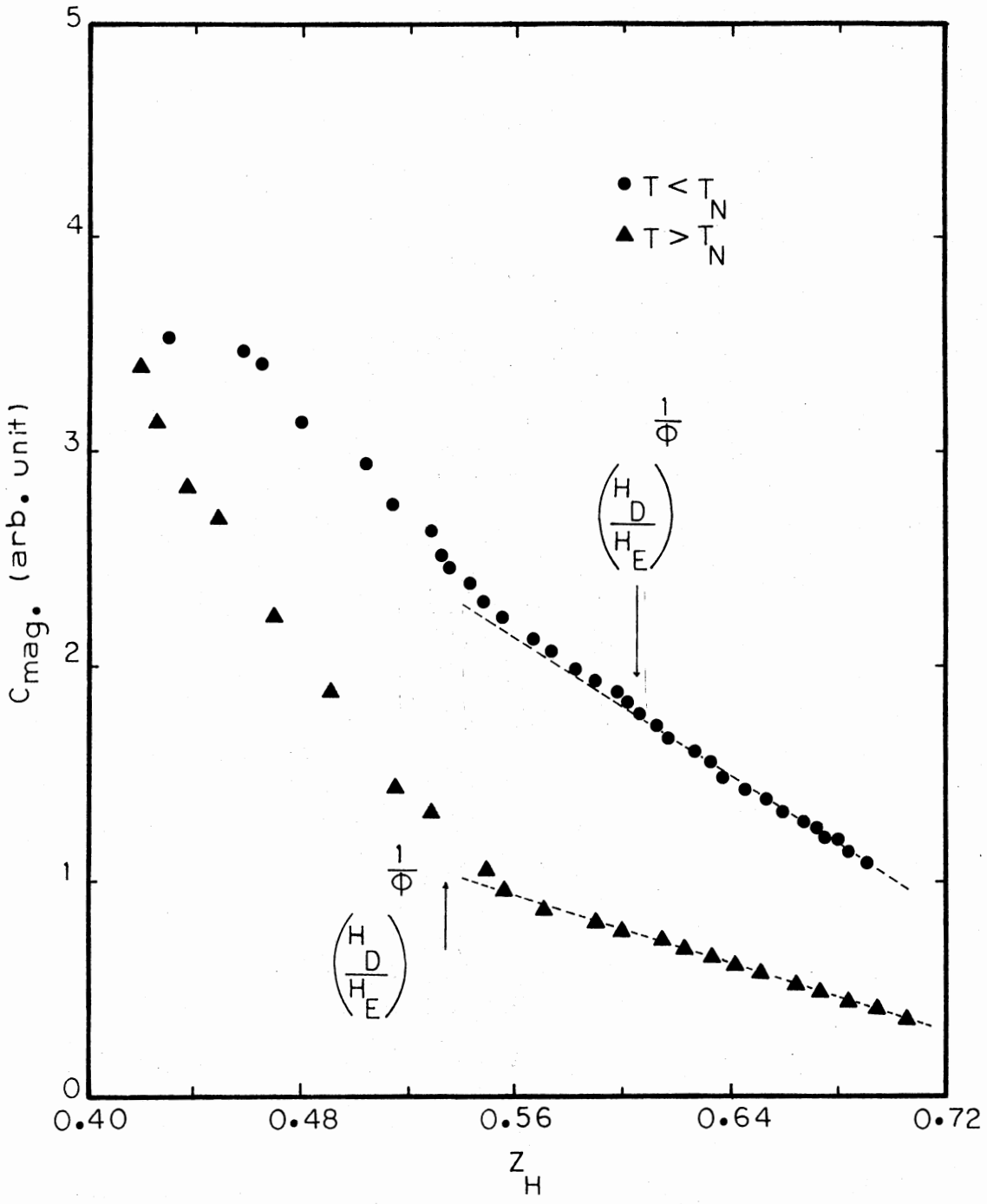

Figure 21. Mag. Specific Heat for 2.92% Zinc Doped Sample Versus $Z_H = (t)^{0.14}\,[1 \pm 0.25(t)^{0.5}]$ Assuming Heisenberg-Behavior

magnetic specific heat versus

$$Z_H = (t)^{0.14} [1 \pm 0.25 (t)^{0.5}] .$$

These results show a very good straight line behavior for $Z_H > 0.605$ ($t > 4 \times 10^{-2}$) for $T < TN$ and $Z_H > 0.534$ ($t > 10^{-2}$) for $T > TN$. It may be worth mentioning that the corrections to scalling are small compared to 1 even for the largest t's in these experiments. They do not suffice to linearize the data on such a plot. For higher concentrations the region $T < 10^{-2}$ is masked by the rounding due to the impurities and these impurity-effects dominate the critical behavior.

Discussion

It is now important to compare our result with the earlier work by Teaney (56), and by Boo and Staut (52). Apparently, these three results seem to be to agree qualitatively. In fact, Teaney and Boo and Staut, analyzing their experimental data concluded that experimental points shows a positive curvature in the logarithmic plot, then the specific heat diverged with a small positive exponent α, that is $0 \leq \alpha < 0.1$. Their conclusion suggests that the specific heat singularity is characteristic of the Ising system, rather than the 3D Heisenberg system which, however, conflicts with the result by neutron scattering study of a direct observation of the critical fluctuation (57).

It should then be of interest to examine the peculiar behavior observed in the present experiment by comparison with the current theories of critical phenomena.

In 1973, Fisher and Aharong (58) have predicted that a crossover

can occur in the Heisenberg magnet with weak dipolar anisotropy at a reduced temperature $|t| = \hat{g}^{\frac{1}{\phi}}$, where $\phi = 1.3$ in 3D magnet and $\hat{g}$ is essentially the ratio of the dipolar field H_D to the exchange field H_E.

A few decades ago, Keffer (59) estimated H_E and H_D for mangenese difluoride at O K. He calculated H_E and H_D as 540,000 Oe and 8300 Oe, respectively. The calculated value for T < TN and T > TN by Ikeda (60) shows

$$|t| = \left(\frac{HD}{HE}\right)^{\frac{1}{\phi}} = 4.0 \times 10^{-2} \quad T < TN$$

$$|t| = \left(\frac{HD}{HE}\right)^{\frac{1}{\phi}} = 9.6 \times 10^{-3} \quad T > TN$$

corresponding to the values $Z_I = 1.42$ for T < TN and $Z_I = 1.83$ for T > TN for Ising-like behavior and $Z_H = 0.605$ for T < TN and $Z_H = 0.534$ for T > TN for Heisenberg-like behaviors.

We can now plausibly explain the peculiar behavior of the critical specific heat observed in our data. The phenomena observed at both T > TN and T < TN can be explained as the corssover from Heisenberg to Ising-like behavior. At T < TN this crossover occur at reduced temper-

$|t| = \left(\frac{H_D}{H_E}\right)^{\frac{1}{\phi}} = 4.0 \times 10^{-2}$ ($Z_I = 1.42$ or $Z_H = 0.605$) and for T > TN at

$|t| = \left(\frac{H_D}{H_E}\right)^{\frac{1}{\phi}} = 9.6 \times 10^{-3}$ ($Z_I = 1.83$ or $Z_H = 0.534$). It may need to be emphasized that this type of crossover has been seen by Birgeneau, Cowely and Shirane (8) in the analysis of neutron scattering experiment

on $Mn_{1-c}\ Zn_c\ F_2$.

Summary and Conclusion

The magnetic specific heat of zinc doped mangenese diflouride was measured for different composition of zinc. The results shows the transition temperature will decrease as the concentration increases. The change in Néel temperature versus zinc concentration is linear as predicted by theory. The analysis of the data is clearly demonstrated that, as we are approaching to transition temperature the system corss-over from isotropic behavior to an anisotropic behavior, or in another word, the system crossover from Heisenberg-like behavior to Ising-like behavior. This crossover is exactly at the point that predicted by theory due to dipolar interaction.

BIBLIOGRAPHY

1. Brout, R., Phase Transitions (W. A. Benjamin, Inc., New York, 1965).

2. Anderson, P. W., Rev. Mod. Phys. 38, 298 (1966).

3. Landau, L. D. and Lifshiz, E. M., Statistical Physics (Pergamon Press, London, 1958), Chapter 14.

4. Sengers, A. L. and J. V. Sengers, C & EN Feature, June 10, 1968.

5. Cooper, M. J. and R. Nathans, J. Appl. Phys. 37, 1041 (1966).

6. Wilson, K. and J. Kogut, Phys. Rep. C12, 76 (1974).

7. Jahn, F. R., J. B. Merkel, G. A. Gehrig and P. J. Becker, Physica 89B, 177-180 (1977) North-Holland.

8. Birgeneau, R. J., R. A. Cowley and G. Shirane, J. Appl. Phys. 50, 1788-89 (1979).

9. Grinstein, G. and A. Luther, Phys. Rev. B13, 1329 (1976).

10. Essam, J. W. and M. E. Fisher, J. Chem. Phys. 38, 802 (1963).

11. Stanley, H. E., Phys. Rev. Lett. 20, 589 (1968).

12. Stanley, H. E., J. Phys. Soc. Japan, 26S, 102 (1969).

13. Fisher, M. E., J. Math. Phys. 5, 944 (1964).

14. Gaunt, D., M. E. Fisher, M. Sykes, and J. W. Essam, Phys. Rev. Lett., 13, 713 (1964).

15. Heller, P. and G. B. Benedek, Phys. Rev. Lett. 8, 428 (1962).

16. Heller, P. and G. B. Benedek, Phys. Rev. Lett. 14, 71 (1965).

17. Weinberger, M. A. and Schneider, Can. J. Chem. 30, 4222 (1952).

18. Domb, C. and M. F. Sykes, J. Math. Phys. 2, 63 (1961).

19. Domb, C. and M. F. Sykes, Phys. Rev. 128, 168 (1961).

20. Gammel, J., W. Marshall and L. Morgan, Proc. Roy Soc. (London), A275 (1963).

21. Baker, G. A., J. Phys. Rev. 136A, 1376 (1964).

22. Jaciot, B., J. Konstantinovic, G. Parette and D. Gribier, Symposium on Inelastic Scattering of Neutron in Solids and Liquid, Chalk River (1962).

23. Noakes, J. E. and A. Arrott, J. Appl. Phys. 35, 931 (1964).

24. Levelt, Sengers J. M. H., Physica 73, 73 (1974).

25. Arajs, S., Conference on Magnetism and Magnetic Materials, J. Appl. Phys. (1965).

26. Kouvel, J. and M. E. Fisher, Phys. Rev. 136A, 1626 (1964).

27. Kadanoff, L. P., Rev. Mod. Phys. 39, 395 (1967).

28. Corliss, J. M., Delapaline, A., J. M. Hasting, H. Y. Lau, R. Nathans, J. Appl. Phys. 40, 1278 (1969).

29. Wortis, M., In Gunton and Green, p. 96 (1973).

30. Barmatz, M., P. C. Hohenberg and A. Kornblit, Phys. Rev. B 12, 1947-68 (1975).

31. Brown, G. R. and H. Meyer, Phys. Rev. A 6, 364 (1972).

32. Kornblit, A., G. Ahlers, Phys. Rev. B 11, 267B (1975).

33. Ahlers, G. and A. Kornblit, Phys. Rev. B 12, 1938 (1975).

34. Reanalysis of Specific-Heat Data of Salamon, M. B. and A. I. Kushima [A.I.P. Conf. Proc. 5, 1269 (1971)].

35. Gaunt, D. S. and C. Domb, J. Phys. C 3, 1442 (1970).

36. Koasnow, R. and H. E. Stanley, Phys. Rev. B 8, 332 (1973).

37. Baker, J. M., J. A. J. Louoens, and R. W. H. Stevenson, Proc. Phys. Soc. 77, 1038-41 (1961).

38. Buchanan, M., W. J. L. Buyers, R. J. Elliott, R. T. Harlep, W. Hayes, A. M. Perry and I. D. Saville, J. Phys. C: Solid State Phys. 5, 2011-25 (1972).

39. Buyers, W. J. L., Pepper, and R. J. Elliott, J. Phys. C: Solid State Phys. b, 1933-51 (1973).

40. Elliott, R. J., B. R. Heap, D. J. Morgan and G. S. Rushbrooke, Phys. Rev. Lett., 5, 366-8 (1960).

41. Coombs, G. J. and R. A. Cowley, J. Phys. C: Solid State Phys. 8, 1889-900 (1975).

42. Coombs, G. J., R. A. Cowley, W. J. L. Buyers, E. C. Svensson, T. M. Holden, and D. A. Jones, J. Phys. C: Solid State Phys. 9, 2167-83 (1976).

43. Holcomb, W. K., J. Phys. C: Solid State Phys. 7, 4299-313 (1974).

44. Tennant, W. E. and P. L. Richards, J. Phys. C: Solid State Phys. 10, L 365-67 (1977).

45. Erickson, R. A., Phys. Rev. 90, 779-85 (1953).

46. Staut, J. W. and S. A. Reed, J. Am. Chem. Soc. 76, 5279 (1954).

47. Wolf, M. W. "The Low Temperature Thermal Conductivity of Potassium Zinc Fluoride" (Unpublished Ph.D. Dissertation, Oklahoma State University, 1974).

48. Sullivan, P. F. and G. Seidel, Phys. Rev. 173, 679 (1968).

49. Handler, P., D. E. Mapother, and M. Rajl, Phys. Rev. Lett. 19, 356 (1967).

50. Carslaw, H. S. and J. C. Jaeger, Conduction of Heat in Solids (Oxford University Press, London, 1959) 2nd Ed. pp. 110ff.

51. Staut, J. W. and E. Catalano, J. Chem. Phys. 23, 2013-2022 (1955).

52. Boo, W. O. and J. W. Staut, J. Chem. Phys. 65, 3929-34 (1976).

53. Barmatz, M., P. C. Hohenberg and Korubit, Phys. Rev. B 12, 1947 (1975).

54. Saul, D. M., M. Wortis and D. Jasnow, Phys. Rev. B 11, 2571 (1975).

55. Rives, J. E. and D. P. Landau, Phys. Rev. B 17, 4426 (1978).

56. Teaney, D. T., Phys. Rev. Lett. 14, 898-900 (1965).

57. Shulhoff, M. P., R. Nathans, P. Heller and A. Linz, Phys. Rev. B 4, 2254-76 (1971).

58. Fisher, M. E. and A. Aharohy, Phys. Rev. Lett. 30, 559-62 (1973).

59. Keffer, F., Phys. Rev. 87, 608-12 (1952).

60. Ikeda, H., N. Okamura, K. Kato and A. Ikushima, J. Phys. C 11, L231-235 (1978).

APPENDIX A

COMPUTER PROGRAM THAT READS THREE CHANNELS

```
1 CONSOLE 18,1 :LIST: CONSOLE 16,1
10 DIM DA(2,600)
20 REM COMPUTER COMMANDS DMM TO MAKE MEASUREMENT
30 REM THEN WHEN DATA IS READY IT IS READ
40 MJ=1
50 PRINT "THE COMPUTER WILL READ THE AC TEMPERATURE, TAC, AND"
60 PRINT " THE MEAN TEMPERATURE OF THE SAMPLE CELL, T"
70 PRINT
80 JJ=1
90 INPUT "THE THREE CHANNELS TO BE READ, TAC FIRST":C1,C2,C3
100 INPUT "THE INTERVAL BETWEEN DATA SETS IN MACHINE CYCLES"; IT
110 OUT 36,O
120 OUT 38,O
130 OUT 37,O
140 OUT 39,111
150 OUT 36,4
160 OUT 38,4
170 OUT 39,255
180 OUT 32,O
190 OUT 34,O
200 OUT 33,O
210 OUT 35,O
220 OUT 32,4
230 OUT 34,4
240 5=O
250 X=1/10
260 Y=1/100
270 Z=1/1000
280 Z1=1/10000
296 Z2=Z1/10
300 CH=C1
310 CK=CH+240
320 OUT 39,CK
330 FOR J=1 TO 75
340 NEXT J
350 OUT 39,CH
360 OUT 39,CK
370 STAT=INP(39)
380 IF STAT>=128 THEN GOTO 370
390 LET A=INP(33)
400 LET B=INP(35)
410 LET G=INP(37)
420 C=INT(A/16)
430 IF A>15 THEN D=A-16
440 IF A<15 THEN D=A
450 E=INT(B/16)
460 IF B>9 THEN F=B-E*16
470 IF B<=9 THEN F=B
480 H=INT(G/16)
490 IF G>9 THEN I=G-H*16
500 IF G<=9 THEN I=G
510 S=C+D*X+E*Y+F*Z+H*Z1+I*Z2
511 STAT =STAT-CH
513 IF STAT >=111 THEN S=-S
```

```
520 DA(1,JJ)=CH
530 DA(2,JJ)=S
540 PRINT JJ,CH,S
550 JJ=JJ+1
551 IF JJ>600 THEN 620
560 IF CH=C1 THEN CH=C2 ELSE 562
561 GOTO 310
562 IF CH=C2 THEN CH=C3 ELSE CH=C1
563 IF CH=C3 THEN 310
570 IF CH=C2 THEN 310
580 FOR J=1 TO IT
590 NEXT
600 PRINT
610 GOTO 310
620 ON MJ GOTO 640,660,680,700,720,740,760,780,800,820,840,860,880
630 PRINT "OUT OF ARRAYS FOR TAPE STORAGE"
631 PRINT ""
632 GOTO 630
640 OSAVE "*DA DA1 :O
650 GOTO 900
660 OSAVE "*DA DA2 :O
670 GOTO 900
680 OSAVE "*DA DA3 :O
690 GOTO 900
700 OSAVE "*DA DA4 :O
710 GOTO 900
720 OSAVE "*DA DA5 :O
730 GOTO 900
740 OSAVE "*DA DA6 :O
750 GOTO 900
760 OSAVE "*DA DA7 :O
770 GOTO 900
780 OSAVE "*DA DA8 :O
790 GOTO 900
800 OSAVE "*DA DA9 :O
810 GOTO 900
820 OSAVE "*DA DA10 :O
830 GOTO 900
840 OSAVE "*DA DA11 :O
850 GOTO 900
860 OSAVE "*DA DA12 :O
870 GOTO 900
880 OSAVE "*DA DA13 :O
900 MJ=MJ+1
910 JJ=1
920 CH=C1
930 GOTO 310
OK
```

APPENDIX B

COMPUTER PROGRAM TO CALCULATE SPECIFIC HEAT

```
1 CONSOLE 18,1 :LIST: CONSOLE 16,1
10 DIM AR(2,600) ,ZZ(2,200)
20 AR=.1686466337#
30 BR=-.09102717295#
40 CR=4.758946595D-03
50 DR=-7.747302235D-05
60 AU=9.784
70 BU=2.283333334D-03
80 CU=-2.6D-04
90 DU=6.666666667D-07
100 AT=8147.51561#
110 BT=-2702.213312#
120 CT=305.9191829#
130 DT=-11.71648754#
140 OLOAD "*AR DA1 :O
141 K=1
150 M=1
160 N=2
170 L=3
175 J=1
180 GOSUB 500
190 OLOAD "*AR DA2 :O
191 K=2
200 M=1
210 N=2
220 L=3
221 J=1
230 GOSUB 500
240 OLOAD "*AR DA3 :O
241 K=3
250 M=1
260 N=2
270 L=3
271 J=1
280 GOSUB 500
290 OLOAD "*AR DA4 :O
291 K=4
300 M=1
310 N=2
320 L=3
325 J=1
330 GOSUB 500
340 OLOAD "*AR DA5 :O
341 K=5
350 M=1
360 N=2
370 L=3
375 J=1
380 GOSUB 500
390 OLOAD "*AR DA6 :O
395 K=6
400 M=1
410 N=2
```

```
420 L=3
425 J=1
430 GOSUB 500
440 OLOAD "*AR DA7 :O
445 K=7
450 M=1
455 N=2
460 L=3
465 J=1
466 GOSUB 500
470 OLOAD "*AR DA8 :O
471 K=8
475 M=1
480 N=2
490 L=3
491 J=1
495 GOSUB 500
500 AR(2,M)=AR(2,M)*100
510 Z=LOG (AR(2,M))
520 TO=AR+BR*Z+CR*Z*Z*Z+DR*Z*Z*Z*Z*Z
530 T=1/TO
540 UO=AU+BU*T+CU*T*T+DU*T*T*T
550 U=UO+AR(2,N)
560 T=AT+BT*U+CT*U*U*DT*U*U*U
600 FT=(BT+2*CT*U+3*DT*U*U)*AR(2,L)
605 KH=1/FT
610 SH=-KH*100
620 PRINT "SPECIFIC HEAT ";SH,"TEMPERATURE ";T
625 PRINT ""
630 M=M+3
640 N=N+3
650 L=L+3
651 IF M>600 GOTO 800
652 ZZ01,J)=SH
653 ZZ(2,J)=T
654 J=J+1
663 IF J<200 THEN 500
664 IF K=1 THEN OSAVE "*ZZ Z1 :1
665 IF K=2 THEN OSAVE "*ZZ Z2 :1
670 IF K=3 THEN OSAVE "*ZZ Z3 :1
680 IF K=4 THEN OSAVE "*ZZ Z4 :1
690 IF K=5 THEN OSAVE "*ZZ Z5 :1
700 IF K=6 THEN OSAVE "*ZZ Z6 :1
710 IF K=7 THEN OSAVE "*ZZ Z7 :1
720 IF K=8 THEN OSAVE "*ZZ Z8 :1
800 RETURN
OK
```

VITA

Hadi Salamati-Mashhad

Candidate for the Degree of

Doctor of Philosophy

Thesis: SPECIFIC HEAT NEAR THE NÉEL POINT IN THE Mn_{1-c} Zn_c F_2 SYSTEM

Major Field: Physics

Biographical:

Personal Data: Born in Mashhad-Iran, September 11, 1948, the son of Mr. and Mrs. M. K. Salamati.

Education: Received Licentiate degree from University of Mashhad-Iran in September, 1972; received Master of Science degree in physics from Oklahoma State University in 1977; completed requirements for the Doctor of Philosophy degree at Oklahoma State University, in May, 1981.

Professional Experience: Graduate Teaching Assistant, Oklahoma State University, 1975-1981.